

# Imperial College London

## FINAL YEAR PROJECT REPORT

IMPERIAL COLLEGE LONDON

DEPARTMENT OF ELECTRICAL AND ELECTRONIC ENGINEERING

---

### An open-source solar-powered street light for off-grid South Africa

---

*Author:*  
Grace Tam  
CID 01560843

*Supervisor:*  
Dr. A. Junyent-Ferré  
*Second Marker:*  
Dr P.R. Clemow

June 22, 2022

### **Final Report Plagiarism Statement**

I affirm that I have submitted, or will submit, an electronic copy of my final year project report to the provided EEE link.

I affirm that I have submitted, or will submit, an identical electronic copy of my final year project to the provided Blackboard module for Plagiarism checking.

I affirm that I have provided explicit references for all the material in my Final Report that is not authored by me, but is represented as my own work.

## **Abstract**

The South African Volunteer Workers Agency (SAVWA) has reached out to Imperial College London to design a PV-powered streetlight for their community centre based in Soshanguve, South Africa. The organization experiences regular power outages in their local municipality, and a PV-powered streetlight would help make the streets by their centre safer at night.

This report presents a system level design of the PV streetlight with in-depth analysis about the voltage and power ratings of each subsystem. Following this, the individual subsystems are designed and implemented. An IC-based design for the charge controller is documented, with the circuit performing MPPT and CC/CV charging. The battery management system is an adaptation of a separate open source project, and the circuit implements cell balancing and overcharge/overdischarge protection. Finally, an LED lightsource is designed, with a dimming functionality controlled by a microcontroller.

## **Acknowledgements**

I would like to thank my supervisor, Dr Adrià Junyent-Ferré, for your patience, guidance and advice throughout my project. I'm especially grateful for your support while getting the hardware working in the final stages of the project.

I also extend my thanks to Dr Philip Clemow for the valuable insight on batteries and the BMS. Thank you to Mr Victor Boddy for your help in soldering the ICs onto the board, your expertise contributed greatly to the work done in this project. Special thanks to Sam for teaching me PCB design, and to Swetha for looking through my circuit with me. I would not have been able to move past certain stages of my project without your help.

To my parents, thank you for your constant support and encouragement throughout my degree and this project. I really could not have done it without your support.

To my friends, thank you for encouraging me and keeping me in prayer. I am so blessed to have all of you in my life.

Soli Deo Gloria.

# Contents

<b>1</b>	<b>Introduction</b>	<b>7</b>
<b>2</b>	<b>Background</b>	<b>8</b>
2.1	System Overview . . . . .	8
2.2	PV Panel . . . . .	9
2.2.1	PV Panel Glossary . . . . .	9
2.2.2	Power Output of PV Panel and MPPT . . . . .	9
2.2.3	Single Diode Equivalent Circuit and Mathematical Background .	11
2.3	Charge Controller . . . . .	12
2.4	Battery Theory . . . . .	13
2.4.1	Battery Glossary . . . . .	13
2.4.2	Battery Chemistry . . . . .	14
2.4.3	CC/CV Charging . . . . .	14
2.4.4	Battery Protection . . . . .	15
2.4.5	Cell Balancing . . . . .	15
2.5	Luminaire . . . . .	16
2.5.1	Lighting Standards . . . . .	16
2.5.2	Efficiency of Luminaire Technologies . . . . .	17
<b>3</b>	<b>Requirements Capture</b>	<b>18</b>
3.1	Initial Sizing . . . . .	18
3.2	Competitor Analysis . . . . .	20
3.3	Project Deliverables . . . . .	21
<b>4</b>	<b>Analysis and System Design</b>	<b>22</b>
4.1	PV Panel . . . . .	22
4.1.1	Selection of PV Panel . . . . .	22
4.1.2	PV Panel Modelling in Simulink . . . . .	23

4.1.3	Simulation of PV Panel Power Output . . . . .	26
4.2	Battery . . . . .	27
4.2.1	Selection of Battery Chemistry . . . . .	27
4.2.2	Series-Parallel Arrangement of Battery . . . . .	28
4.2.3	Battery Management System . . . . .	29
4.3	Charge Controller . . . . .	31
4.4	Luminaire . . . . .	33
4.5	Revised System Sizing . . . . .	35
<b>5</b>	<b>Subsystem Implementation</b>	<b>37</b>
5.1	Charge Controller . . . . .	37
5.1.1	Circuit Design . . . . .	37
5.1.2	LTSpice Simulation . . . . .	39
5.1.3	Evaluation Board . . . . .	41
5.1.4	PCB Design . . . . .	42
5.2	Battery Management System . . . . .	44
5.3	Luminaire . . . . .	47
<b>6</b>	<b>Testing</b>	<b>48</b>
6.1	Charge Controller . . . . .	48
6.1.1	Setup . . . . .	48
6.1.2	Validation of CC/CV Charging . . . . .	50
6.1.3	Validation of MPPT . . . . .	50
6.1.4	Efficiency . . . . .	52
6.2	Battery Management System . . . . .	53
6.2.1	Setup . . . . .	53
6.2.2	Voltage Measurement Circuit . . . . .	54
6.2.3	Cell Balancing Circuit . . . . .	56
<b>7</b>	<b>Conclusion and Further Work</b>	<b>59</b>
7.1	Conclusion . . . . .	59
7.2	Further Work . . . . .	59
<b>A</b>	<b>PV Panel Spice Model</b>	<b>62</b>
<b>B</b>	<b>Bill of Materials</b>	<b>63</b>
B.1	Charge Controller . . . . .	63
B.2	BMS . . . . .	64

B.3 Miscellaneous . . . . .	65
-----------------------------	----

# List of Figures

2.1	An overview of the PV streetlight system . . . . .	8
2.2	I-V and P-V curves for various irradiance and temperatures . . . . .	10
2.3	Single Diode Equivalent Circuit Source: Sandia National Laboratories [1]	11
2.4	Batteries in series without cell balancing. Source: Analog Devices [2] . . .	15
3.1	Method of determining streetlight's illumination radius . . . . .	19
4.1	Simulink Dialog Box for PV parameter input . . . . .	24
4.2	Simulink Model To Obtain Maximum Power Point . . . . .	25
4.3	2D MPP Lookup Table of Victron 30W Panel . . . . .	25
4.4	Simulink block diagram to input temperature and irradiance into lookup table . . . . .	26
4.5	Daily PV Panel Output in 2015 . . . . .	27
4.6	Categorisation of BMS ICs . . . . .	30
4.7	RECOM LED Driver . . . . .	34
4.8	Full System Level Design . . . . .	36
5.1	Charge Controller Circuit Schematic . . . . .	37
5.2	Charge Controller LTSpice Circuit [3] . . . . .	40
5.3	Simulation of Charge Controller . . . . .	41
5.4	Options for evaluating LT3652 . . . . .	41
5.5	Evaluation of LT3652 using Sparkfun Board . . . . .	42
5.6	Charge Controller PCB . . . . .	43
5.7	Assembled Charge Controller Board . . . . .	43
5.8	Cell Balancing Circuit . . . . .	44
5.9	Cell Balancing PCB . . . . .	46
5.10	Assembled BMS . . . . .	46
5.11	LED PCB . . . . .	47

6.1	Setup of controlled environment for testing charge controller . . . . .	48
6.2	Implementation of charge controller testing environment . . . . .	49
6.3	Graph of CC/CV charging at peak power conditions . . . . .	50
6.4	Charge controller setting the operating point of the PV panel . . . . .	51
6.5	Charge controller MPPT under varying irradiance . . . . .	52
6.6	Charge controller efficiency across different battery voltages . . . . .	53
6.7	Resistor ladder used to mimic cell voltages . . . . .	54
6.8	Test setup of BMS with resistor ladder to emulate the battery voltages . .	54
6.9	Graph of actual cell voltage plotted against ADC reading of microcontroller for calibration of voltage reading circuit . . . . .	55
6.10	Graph of cell voltages read by multimeter and microcontroller . . . . .	56
6.11	Graph of balancing current at each cell for a range of battery voltages . .	57
6.12	Temperature profile of bleeding resistors when cell 3 has the lowest voltage	58
7.1	Alternative system design for reduced cost and reduced reliability . . . . .	61
A.1	Single Diode PV LTSpice Model . . . . .	62

# List of Tables

3.1	Design specifications of system . . . . .	20
3.2	Specifications of other products on the market . . . . .	20
4.1	Comparisons of 30W PV Panels . . . . .	23
4.2	Comparisons of Battery Chemistries . . . . .	28
4.3	BMS Specifications . . . . .	29
4.4	Comparison of Charge Controller ICs . . . . .	32
5.1	Minimum component values and ratings as advised by LT3652 datasheet .	39
B.1	Charge Controller Bill of Materials . . . . .	64
B.2	BMS BOM . . . . .	65
B.3	Bill of Materials for the system . . . . .	65

# Chapter 1

## Introduction

Off-grid electrification has a lot of applications in areas where the supply of electricity is unreliable. South Africa has been experiencing an energy crisis since 2007 whereby the country experiences regular power cuts as a result of load shedding [4]. In 2019, the country experienced the worst blackouts, with a period where more than a third of the national service provider's capacity was cut off [5].

Proper lighting of public areas like roads and community squares is vital for the safety and wellbeing of communities, both in urban and rural areas. There is a 30% decrease in traffic accidents on roads that are well lit [6], and pedestrians also benefit from street lighting as it makes walking home at night safer.

There has been a great uptake for PV-powered streetlights in South Africa in the past 5 years, but the products are either too expensive for communities in rural areas to afford, or cheap but poor in quality. An initial study of professionally designed solar streetlights in South Africa put the price range of each light between £200- £600. The cost and logistics of repair are also taken into consideration – if a part becomes spoilt, it is not easy to get the PV panels repaired which might result in the other working parts being thrown away.

It would benefit communities in rural areas around the world and volunteer agencies if there are more affordable PV powered streetlights on the market. Besides that, if they have access to open-sourced design files such as PV panel sizing and charge controller PCB design files that can be downloaded and sent to manufacturers near the region, they can save on a lot of logistics cost.

# Chapter 2

## Background

### 2.1 System Overview

This project begins with a literature review of PV-powered streetlights to provide context about the system architecture. A common PV system design was found to be: a PV panel, charge controller, battery and load (which is a light-source in this project) [7] [8]. The system overview is summarised in Figure 2.1.

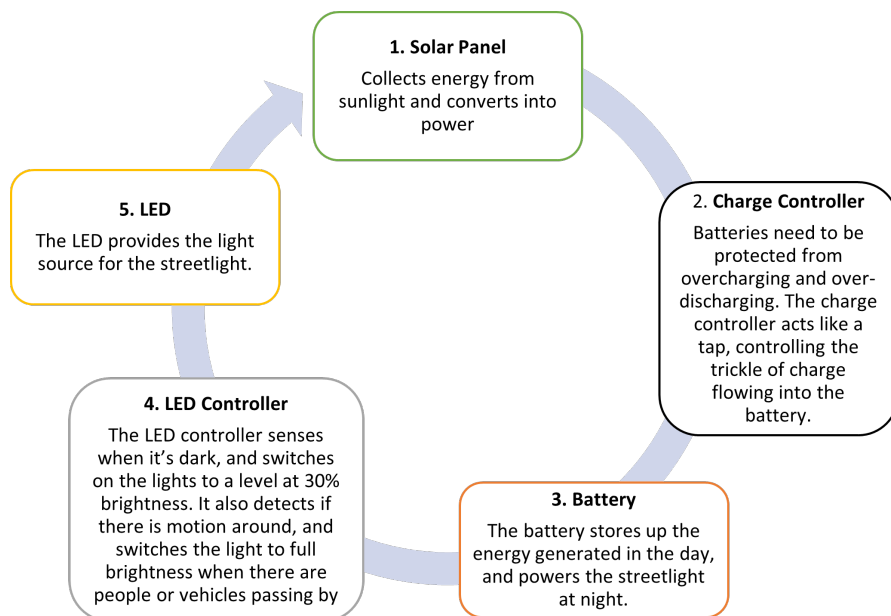


Figure 2.1: An overview of the PV streetlight system

During the literature review, a few similar masters and bachelors level thesis were also

identified [9, 10]. [9] focuses on the need for streetlighting and discusses in depth background theory about lighting, however the design sections are redacted so there is no danger about similarities. [10] is the only report out of the two that has circuit designs. It discusses the design of the charge controller but does not go in-depth about the functions of the IC or the design of the PCB. Besides that, there is no discussion about the system sizing.

## 2.2 PV Panel

### 2.2.1 PV Panel Glossary

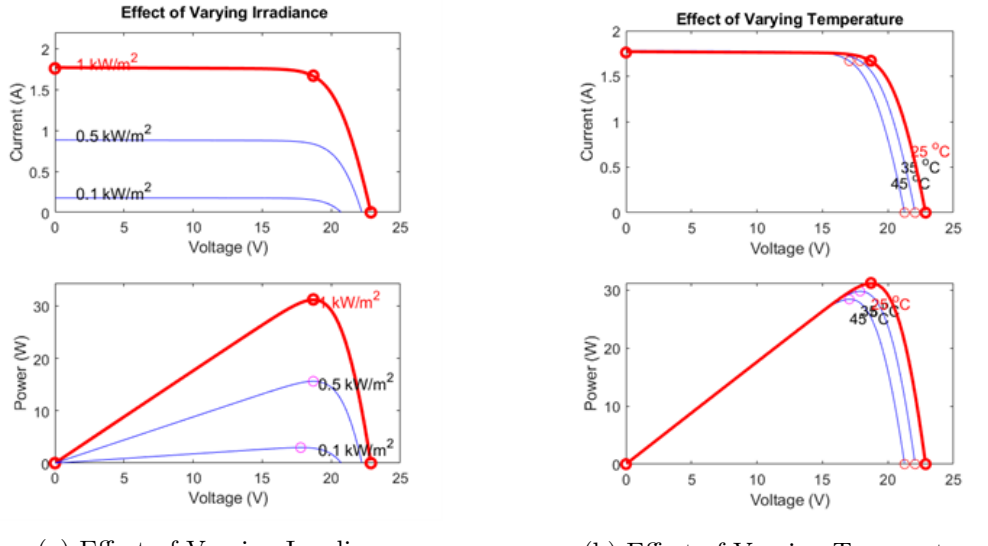
PV cells act as the power source, converting solar energy into usable electrical energy. There are different types of PV cells available such as monocrystalline or polycrystalline cells, but monocrystalline cells produce more power given the same conditions. PV cells are joined in series or in parallel to form what is known as a PV panel. A few concepts vital to the discussion of solar power and PV technology need to be introduced:

- **Solar Radiation:** The energy emitted by the sun [11].
- Irradiance: The total radiated power received by an object per unit of surface [11].
- **Global Horizontal Irradiance:** The total radiated power received by a horizontal surface. This parameter is often used in discussions about fixed solar panels [12].
- **Direct Normal Irradiance:** The total radiated power received by a surface perpendicular to the direction of radiation. This parameter is used when discussing solar-tracking PV panels [12].

### 2.2.2 Power Output of PV Panel and MPPT

The two main factors that determine the power output of the PV panel are the irradiance and temperature. Each IV curve describes the output current and voltage characteristic when external conditions like irradiance and temperature are held constant. Increasing the irradiance shifts the entire IV curve vertically, while increasing the temperature shifts the curve to the left. In layman's terms, the power output of a solar panel is highest on a sunny and cold day. [7]

Another factor that influences the power output is the air mass (AM). For the solar radiation to reach the PV panel, it must first travel through the atmosphere where the



(a) Effect of Varying Irradiance

(b) Effect of Varying Temperature

Figure 2.2: I-V and P-V curves for various irradiance and temperatures

energy gets scattered or absorbed. The longer the path the sun beam takes, the more energy is lost to the atmosphere. This path is known as the air mass, and the minimum air mass is defined to be AM1 which is a path vertical to sea level [13].

Besides that, the tilt angle of the PV panel determines how much of the available irradiance it can capture. Ideally, the PV panel should be directed in such a way that its surface receives the sun beams vertically. Some systems employ a tracker such that the PV panel is always directed towards the sun, however this adds cost and complexity of maintenance. For a fixed PV panel, the angle at which it receives solar radiation changes as the position of the sun changes through the day. In this situation, the effective area of the PV panel is a derated value of area to describe how much surface is actually receiving the solar radiation. The effective area is maximum when the solar radiation is directed vertically towards it. [13]

We can also see from the IV curve that there are many possible combinations of output voltages and output currents. Since the power is the product of output voltage and current, this means there are many possible power outputs for each given external condition. The best scenario for power generation is to be operating at the maximum power point ( $V_{MP}, I_{MP}$ ), and this is achieved by setting the load voltage to be  $V_{MP}$ , for example using a DC-DC converter.

The power generating capacity of the PV panel is characterised by its Watt Peak, which is the maximum power output under Standard Test Conditions (STC). These conditions are an irradiance of  $1000W/m^2$ , temperature of  $25^\circ C$ , and air mass 1.5, and are used when benchmarking PV panels [11]. STC is considered to be an overly optimistic test condition, which means the power output of the PV panel will be much lower than expected.

With the irradiance and temperature changing throughout the day and the power output quoted on PV datasheets being too optimistic, the energy available per day cannot be determined on the basis of multiplying the Watt-Peak by the hours of sunlight. Though this provides a starting point for calculations, a more accurate method of sizing the PV panel is obtained through simulations.

### 2.2.3 Single Diode Equivalent Circuit and Mathematical Background

There are several equivalent circuit models for a PV cell, and one of the most widely used circuits is the single-diode equivalent model [1], due to its simplicity and accuracy. Another alternative is the two-diode model; however, this adds complexity that is unnecessary for our application.

$I_L$  is the light-generated current which models the current within the PV cell that is generated from the solar energy received.  $I_D$  represents the current flowing through the parasitic diode that is created because of the pn junction. The shunt resistance  $R_{sh}$  and series resistance  $R_s$  model the power losses of the PV cell.

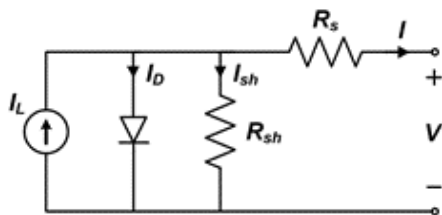


Figure 2.3: Single Diode Equivalent Circuit  
Source: Sandia National Laboratories [1]

The following equations govern this model [1, 14]. The output current  $I$  is the current

that flows through the external circuit, and is calculated using Kirchoff's Current Law:

$$I = I_L - I_D - I_{sh} \quad (2.1)$$

The diode current is modelled by the Shockley equation:

$$I_D = I_0 \left[ \exp \left( \frac{V + IR_s}{nV_T} \right) - 1 \right] \quad (2.2)$$

The current flowing through the shunt branch is calculated using Ohm's Law:

$$I_{sh} = \frac{V + IR_s}{R_{sh}} \quad (2.3)$$

The full equation for the output current in the single diode model is then:

$$I = I_L - I_0 \left[ \exp \left( \frac{V + IR_s}{nV_T} \right) - 1 \right] - \frac{V + IR_s}{R_{sh}} \quad (2.4)$$

The 5 parameters required for this model are [1, 14]:

- The light-generated current,  $I_L$
- The diode reverse saturation current,  $I_0$
- The series resistance,  $R_s$
- The shunt resistance,  $R_{sh}$
- The diode ideality factor,  $n$

## 2.3 Charge Controller

The charge controller protects batteries by controlling the charging current to perform CC/CV charging [15]. Charge controllers fall into two categories: pulse-width modulation (PWM) and maximum power point tracking (MPPT). PWM controllers only adjust the charging current, but do not set the load voltage seen by the PV panel. In other words, there is no DC-DC voltage conversion in PWM controllers. Thus, the load voltage seen by the PV panel would be the nominal voltage of the batteries. The drawback of this design is that the nominal voltages of batteries are usually a lot lower than the maximum power point voltage of the PV panel, so the PV panel would generating

much lower power than what is possible. MPPT charge controllers are able to set the operating point of the PV panel to be equal to  $V_{MPP}$ . The ability to extract maximum power makes the MPPT charge controllers more efficient. [16].

MPPT charge controllers typically contain a DC-DC converter to interface the voltage levels, and a microcontroller. The microcontroller controls the charging current and PV operating point based on the state of charge of the battery [17]. In constant current mode, an MPPT algorithm is employed to identify the  $V_{MPP}$  as the irradiance and temperature changes throughout the day [18]. If the state of charge is above a certain threshold, the output voltage of the PV panel is increased beyond  $V_{MPP}$ , whereby the output current drops drastically thus reducing the charging current [17]. In theory, this should prevent the batteries from being charged beyond their maximum voltage.

## 2.4 Battery Theory

### 2.4.1 Battery Glossary

Batteries are very complex devices that can store and release charge in a circuit. Before discussing the types of batteries and the complexity involved with each, a glossary of battery terminology is first provided. Most of these definitions are taken from [7], which is a very comprehensive guide on PV systems and battery design.

- **Voltage:** A battery's voltage changes according to its state of charge, and the specific voltage-state of charge profile is dependant on the chemistry used in the battery. There are always maximum and minimum voltages where a battery can safely operate at. [7]
- **Nominal Voltage:** Batteries are quoted in terms of their nominal voltage. The nominal voltage of a battery is the voltage that the user can expect the battery to maintain for most of its usage. [7]
- **Capacity:** The capacity of a battery is usually given in amp-hours (Ah). A 10Ah battery would be able to supply 10A for 1 hour, or 5A for two hours, and so on. It also defines the time needed to charge the battery at a given charging current. [7]
- **State of Charge:** The state of charge refers to the amount of charge that the battery has, given as a percentage of its full capacity. [7]

- **Depth of Discharge:** The depth of discharge is the maximum the battery should be discharged. In most batteries, a 100% depth of discharge is not possible as it would severely damage the battery and can cause explosions. Protections need to be put on the battery to prevent it from discharging beyond the limit. The specific threshold is dependant on the battery chemistry and is usually given by battery manufacturers. [7]
- **Cycles:** With rechargeable batteries, the cycles refer to the number of times the battery can be charged and discharged before needing to be replaced. This also depends on the handling of the batteries, as the conditions experienced by the battery affects how long it can be used. For example, a battery can be rated for 3000 cycles at 80% DoD and 2500 cycles at 90% DoD. [7]

#### 2.4.2 Battery Chemistry

Batteries have different characteristics depending on the type of chemistry used to store charge. Of the many different chemistries, a few stand out as being widely used in commercial products. These are the lead acid, gel and lithium batteries. [19]

Lead acid and gel batteries appear to be more affordable than lithium batteries, but they have a lower cycle count. In time, they will need to be replaced and this operating cost adds to its effective cost. Besides that, they have a lower DoD which means the energy that actually produce is lower than the quoted amount. To supply 100Wh at 50% DoD, a 200Wh battery will need to be used. This also adds to the total cost of the battery. [19]

Lithium ion batteries have a longer lifetime and a larger depth of discharge compared to lead acid and gel batteries. However, lithium batteries are less safe as they can explode if mishandled or subjected to stress. In comparison, lead acid batteries are more robust and safer to handle [19]. Lithium Iron Phosphate (LiFePO<sub>4</sub>) is a solution to the problem of lithium battery safety. They have very similar characteristics as other lithium ion cells, but have the advantage of added safety. They are more stable and do not explode even if subjected to physical stress. These advantages do come at a cost, as LiFePO<sub>4</sub> cells are the most expensive out of the battery chemistries. [19, 20]

#### 2.4.3 CC/CV Charging

Lithium batteries, including LiFePO<sub>4</sub>, require a specific charging profile known as constant current-constant voltage (CC/CV) charging. In constant current mode, the battery

is charged at the maximum charging current. Once the battery reaches its maximum voltage, the charging current is reduced to a rate that will keep the battery at a constant voltage. [15]

#### 2.4.4 Battery Protection

Lithium batteries require special protection circuits to prevent damage to the batteries. The conditions that the battery should be protected from are overcharge, overdischarge, and over-current [21]. The battery's voltage is an indication of its SoC, and LiFePO<sub>4</sub> batteries must not be charged beyond 3.65V or discharged below 2.5V [22].

#### 2.4.5 Cell Balancing

Slight variations in the manufacturing of batteries mean that no two cells are the same. Each cell charges at a slightly different rate, and these small deviations can build up over many charging cycles. When batteries are placed in series, there is no mechanism to distribute the charge between batteries so that they maintain a common level of charge throughout their life cycle. Two problems can arise from this. If the stack of batteries are designed to stop being charged at the full stack voltage (eg. 14.4V for a 4s LiFePO<sub>4</sub> arrangement), voltage differences between cells mean that one cell could already be above its individual maximum voltage of 3.6V. A naive way to solve this safety risk would be to check the individual voltages of each cell and stop the charging when any one cell reaches its maximum voltage. However, this reduces the usable capacity of the batteries as the other cells with lower voltages would be cut off before they reach their full SoC. [2]

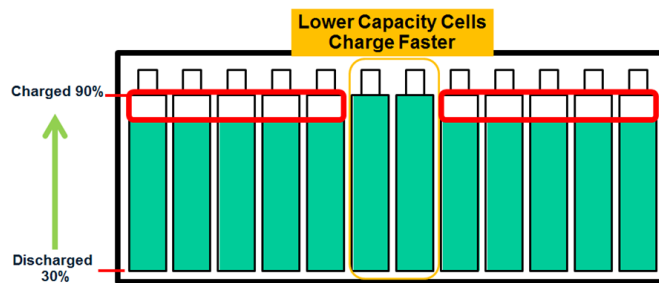


Figure 2.4: Batteries in series without cell balancing.  
Source: Analog Devices [2]

A cell balancing circuit resolves this problem by either distributing the charge between cells in series, or dissipating power from cells with a higher voltage to standardize the

voltages. The former is known as active balancing and the latter is known as passive balancing. Active balancing transfers excess charge from one battery cell to another, which is very energy efficient as no power is wasted. Passive balancing discharges cells through a resistors in a technique known as 'bleeding' current. The current is converted to heat as it passes through the resistor. [2]

Though active balancing is good for the power requirements of the battery pack, the circuits are more complex and expensive than passive balancing circuits. For applications where there is some leeway in the energy capacity, passive balancing is a better alternative. [23]

## 2.5 Luminaire

### Lighting Glossary

The luminaire is the light source of the streetlight and will determine the load that the PV system will need to drive. We begin with a glossary of lighting terminology:

- **Luminous Flux,  $\phi$ :** The amount of light emitted from a light source. Measured in units of lumens [24]
- **Illuminance,  $E$ :** The luminous flux that reaches the surface. Measured in units of lux. [24]
- **Horizontal illuminance:** “The amount of light landing on a horizontal surface such as a desk” [25]
- **Vertical Illuminance:** “The amount of light landing on a vertical surface such as a wall” [25]

#### 2.5.1 Lighting Standards

In the discussion about the brightness received, the illuminance is considered. The amount of light needed in an area depends on many factors. For example, an industrial site would need much brighter lights than a community park since there are heavy duty tools being used. And while bright lights assure that people can see better at night, overly bright lights can cause harm to the community by disrupting people's sleep and contributing to light pollution.

Many countries have developed their own set of lighting standards that state the minimum and maximum illuminance in a given location. For example, the South African standard for public lighting is SANS 10098 [26, 27, 28]. The type of street where the PV powered streetlight will be installed is a residential street with medium to high volume traffic which falls under category B2 of SANS 10098 [28]. This requires a minimum average horizontal illuminance of 5 lux [28, 27].

### 2.5.2 Efficiency of Luminaire Technologies

The conversion from lux to lumens depends on the position and distance of the luminaire, while the conversion from lumens to watts depends on the efficiency of the luminaire.

The energy efficiency of a luminaire is its ability to convert electrical energy into light and is measured in lumens per watt ( $lm/w$ ). Older technologies like mercury vapor lamps have very low efficiencies of between 13–48  $lm/w$ . The technology improved over the years, with high pressure sodium lamps achieving between 60-100  $lm/w$ . The most efficient luminaires to date are light emitting diodes (LED) that have efficiencies ranging from 70 to 150  $lm/w$ . A more detailed comparison of luminaires is available in [29]. Some countries have implemented minimum efficiency requirements, and one such country is South Africa that specifies a minimum of 90  $lm/w$ .[30].

# Chapter 3

## Requirements Capture

### 3.1 Initial Sizing

*'How bright should the streetlight be?'*

This question formed the starting point for discussions surrounding the sizing and ratings of the system. As there were no technical specifications for this project, the lighting requirements of the streetlight first need to be defined. To meet the requirements of SANS 10098 (Section 2.5.1), the minimum horizontal illuminance,  $E$  should be 5 lux. This is the light that is received at ground level. For the design of the luminaire, this must be converted to luminous flux which is the light emitted from the source. This conversion from illuminance to luminous flux,  $\phi$  is performed according to the inverse square law [28]:

$$\phi = E \times 4\pi r^2 \quad (3.1)$$

The streetlight is designed for roads with pedestrian traffic and not large highways that require high streetlight poles. For pedestrian traffic, a height of 3m is sufficient to illuminate the area. Besides that, keeping the height at 3m avoids the need for a complex and expensive installation process. A vertical height of 3 metres corresponds to a spherical radius of 5 metres, as illustrated in Figure 3.1

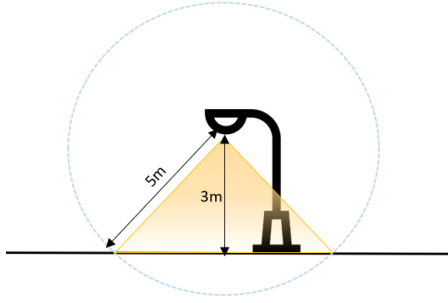


Figure 3.1: Method of determining streetlight's illumination radius

For a spherical radius of 5m, the luminous flux of the light-source should be:

$$\phi = 5 \times 4\pi 5^2 = 1570 \text{ lm} \quad (3.2)$$

To account for any non-idealities and the beam angle of the streetlight, the illuminous flux is increased to 2100 lm. The power needed to supply 2100 lm with 100 lm/w LEDs is calculated by diving the illuminous flux by the efficiency of the LED:

$$P = \frac{2100 \text{ lm}}{100 \text{ lm/w}} = 21 \text{ W} \quad (3.3)$$

The streetlight will be alternating between 30% brightness (low power mode) and full brightness when people walk past it. This load pattern would be very difficult to calculate and simulate as it would require empirical data about the foot traffic of the area where the streetlight is to be installed. Instead of following a specific load pattern, the system will be designed with the target of operating at full brightness for 6 hours a day. Any power saving that comes from 'low power mode' would contribute to the power reserves for the next day. For 6 hours of operation, the required energy is:

$$\text{Demand} = 21 \text{ W} \times 6 \text{ h} = 126 \text{ Wh} \quad (3.4)$$

During the streetlight's operation, this energy would be supplied by the battery. Designing for a 85% depth of Discharge (DoD), the battery capacity can be calculated:

$$\text{Capacity} = \frac{126 \text{ Wh}}{0.85} = 150 \text{ Wh} \quad (3.5)$$

South Africa gets 5 hours of peak sunlight a day [31], and the PV panel needs to produce

150Wh during this time. The estimated size of the PV panel is then:

$$PV = \frac{150Wh}{5h} = 30W \quad (3.6)$$

The technical specifications determined in the initial calculations are summarised in Table 3.1. These specifications are rather pessimistic as large derates were added to the luminaire to allow for inefficiencies and any oversights in the initial sizing. It is expected that the revised sizing would make changes based on the information revealed during the analysis and design stage.

Specification	Value
LED Power	21 W
LED Flux	2100 lm
Battery Capacity	150Wh
PV Panel Rated Power	30W
Charging Time	5 hrs
Runtime	6 hrs

Table 3.1: Design specifications of system

## 3.2 Competitor Analysis

A competitor analysis is introduced at this stage of the report to check if the initial calculations made are within the correct range. Three solar streetlights with similar LED power ratings were compared in Table 3.2. These products are available for purchase in South Africa and the prices were converted from South African Rand to British Pound.

	Solar Streetlights Africa [32]	Solux [33]	Philips SunStay [34]
Brightness	3020 lm	2400 lm	3000 lm
LED Size	20W	20W	17W
PV Peak Power	80 Watt	50W	30W
Battery Size	384 Wh	18 Ah	256 Wh
Runtime	13 hours	20 hours	-
Backup Power	3 days	-	-
Charging time	5 hours	-	5-8 Hours
Price	£326.33	£280.85	£649.71

Table 3.2: Specifications of other products on the market

The first thing to be noted from Table 3.2 is the price of the streetlights. The products range from £280.85 to £649.71. The main reason for the high prices is the backup power that these streetlights are designed to provide. They are designed to run for a minimum of 13 hours, with 3 days worth of backup power in case there is not enough sunlight on certain days. As such, the battery sizes and PV panel peak power are also larger, and this contributes to the cost.

It can be inferred that these products are designed for use in locations like key intersections or off-grid camping where the high reliability is needed. However, not all communities have the means to pay for the added security of supply. This is one area where a trade-off can be made in our design. By making an allowance for a few days per year where there is insufficient sunlight to power the streetlight, the costs can be driven significantly lower.

### 3.3 Project Deliverables

The project's main objective is to develop a set of open-source design files with accompanying instructions on the assembly and repair of the PV-powered streetlight. The user would only need to order the PV panel and LED luminaire according to the specifications, and they would send the PCB file to a manufacturer without needing to open the file to edit it. If one of the hardware components fails due to wear-and-tear, the user would only need to replace that part, and they have all the necessary files to do so. Therefore, the design files will all be end-stage files that are ready for manufacture. The list of files are as follows:

- Bill of materials (including specifications on sizing of PV panel and LED luminaire)
- PCB Gerber files for charge controller
- Code to be uploaded to the microcontroller

## Chapter 4

# Analysis and System Design

The initial sizing provides a good starting point for the system requirements but leaves many blind-spots in the design. Further analysis into the following areas needed to be performed before the individual subsystems and circuits could be implemented. The areas of analysis are:

- Validation of the estimated PV panel size.
- Voltage levels of each subsystem.
- Current flows between each subsystem.
- Evaluation and selection of methods of implementation.

By ironing out the details of the voltage and current levels early in the design, the compatibility of each subsystem can be guaranteed. The background reading in Section 2 hinted at several possible methods of implementing each subsystem, but there was insufficient information about the cost, complexity and availability of each method. An in-depth analysis at this stage would prevent problems like over-complexity or out-of-stock key components from derailing the project in the implementation stage.

### 4.1 PV Panel

#### 4.1.1 Selection of PV Panel

The analysis and design of the PV panel centers around validating the estimated PV panel size that was calculated in Section 3.1. This section heavily draws from the

background information about PV panels and the single diode model that are provided in Section 2.2.

In Section 3.1, the PV size was estimated at 30W. However, the peak power of the PV panel is quoted at STC and real conditions are unlikely to produce a constant power of 30W. This means a 30W PV panel will usually produce less than 30W. To understand the real power output of a PV panel, the PV panel should be simulated with real irradiance and temperature data. This would allow for the validation of the estimated PV panel size. The two things that are needed for this simulation are the PV model and irradiance and temperature data at Soshanguve.

The first step is to select a PV panel to model. 3 PV panels with a peak power of 30W are compared in Table 4.1 and the information provided in each datasheet is listed. The panel produced by Victron under the BlueSolar subsidiary is the cheapest of the three and is selected for this design.

	Victron (Blue Solar) [35]	Renology [36]	RS Pro [37]
Watt Peak (STC)	30W	30W	30W
Efficiency	-	21%	17%
Price	£34.65	£39.99	£64.942
Weight	2.2kg	2.9kg	-
$V_{MPP}$	18.7v	19.5	17.5
$I_{MPP}$	1.61	1.6	1.72
$V_{oc}$	22.87v	22.9	22
$I_{sc}$	1.76A	1.7	1.9

Table 4.1: Comparisons of 30W PV Panels

#### 4.1.2 PV Panel Modelling in Simulink

The next step is to develop the model based on the theory discussed in Section 2.2.3.

[38] describes and compares the three methods of mathematical, circuitry and functional block modelling in Matlab/Simulink. In mathematical modelling, the equations in Section 2.2.3 are put into a Matlab script or a data flow diagram in Simulink. The circuitry method involves building the single diode equivalent circuit in Simulink and using it as a block. The functional block method uses the PV module included in Simulink's PV Array library, which is a ready built model of a PV panel. The paper includes step-by-step instructions on each of the methods implementation, complete with code snippets

and circuit diagrams. It also discusses the pros and cons of each method, with mathematical modelling offering the highest level of control but also being the most complex to implement. The functional block method and the circuit diagram method are easy to implement but has fewer modelling parameters. [38]

For this project, the functional block method is chosen due to its simplicity of implementation. The first step is to define the PV parameters in the dialog box shown in Figure 4.1. The Simulink library contains parameters for an extensive list of PV panels from NREL's database [38]. There is also the option to select 'user defined' in the module selection, which allows the user to build a model for a PV panel that is not included in the database. In this example, a user-defined module is created for the Victron BlueSolar 30W Monocrystalline panel. After the user enters the module data in the left hand side of the dialog box, the 5 parameters needed for the single diode equivalent circuit is calculated based on an optimization algorithm from NREL [38], and is displayed on the right hand side of the dialog box.

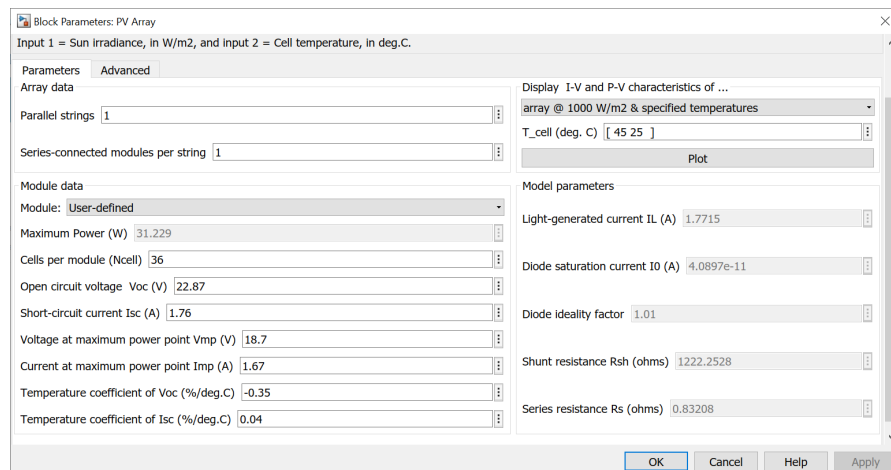


Figure 4.1: Simulink Dialog Box for PV parameter input

After defining the PV module, it can be added to the Simulink workspace. The block diagram in Figure 4.2 is developed based on a design by [38]. In this design, the output voltage is increased from 0 to  $V_{oc}$  using a ramp function to vary the load. The implementation in Figure 4.2 is a slight adaptation from [38] where the output block calculates the maximum power point instead of plotting an IV curve.

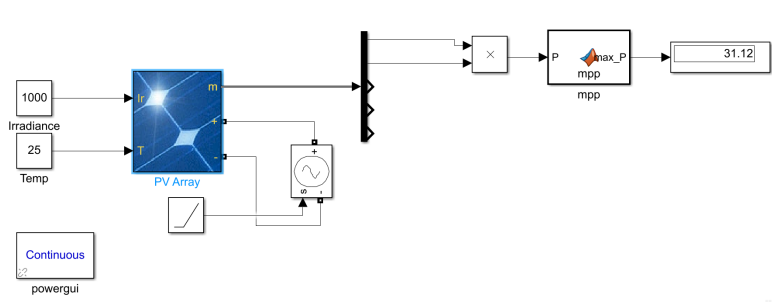


Figure 4.2: Simulink Model To Obtain Maximum Power Point

### MPP Lookup Table

The models developed in this section will be used to simulate the power output with a year's worth of hourly irradiance and temperature data, which amounts up to 8760 calculations. Instead of using the full model in Figure 4.2 for each calculation, the computational complexity can be reduced by creating a look up table to model the PV panel.

If the panel is assumed to be operating at peak performance, then we can take the maximum power point value to be the power output for a given irradiance and temperature. An MPPT algorithm can be added in the subsequent design stages of this project to ensure the panel is operating as close to peak performance as possible. By collecting this peak value for several given irradiances and temperatures, a lookup table based model can be developed. This has been tested [39] and the results were shown to perform better than a conventional model. An example of the Victron BlueSolar MPP Lookup Table is generated for this project and is shown in Figure 4.3.

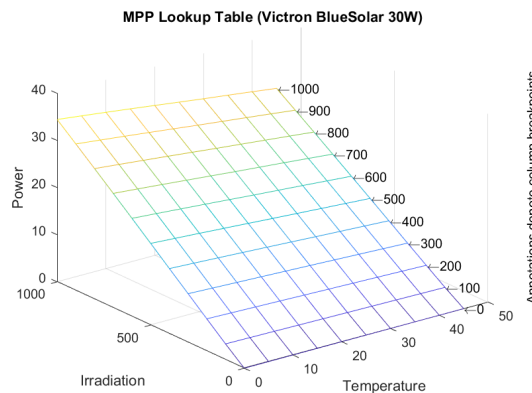


Figure 4.3: 2D MPP Lookup Table of Victron 30W Panel

The lookup table then takes in the daily irradiance and temperature data and identifies the maximum power associated with the given inputs. The output of this block (`out.simout`) is a time series object that contains the hourly power output of the PV panel. This data can then be used to produce graphs of daily energy production.

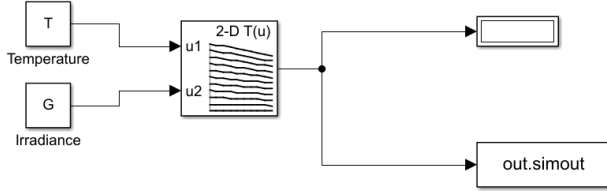


Figure 4.4: Simulink block diagram to input temperature and irradiance into lookup table

#### 4.1.3 Simulation of PV Panel Power Output

The irradiance and temperature data for South Africa were taken from PVGIS [40] which is an online database available to the public. The specific data for Soshangueve was obtained by specifying the coordinates. The dataset was used as input to the PV Panel Model to generate hourly values of power output. From this, the hourly power outputs are summed up to provide the generation output of each day in 2015. This was then visualized by plotting the daily power generation in Figure 4.5.

There are two characteristics in the graph. Firstly, a seasonal trend can be observed. South Africa experiences 4 seasons and as longer days during summer but shorter days during winter. It is very clear that the generation capacity follows this trend with higher outputs during summer (Dec – Feb) and lower outputs during winter (June-Aug). The second feature of the graph is the spikes seen scattered throughout the year. These are the days where energy production is low due to clouds or shading. The total days whereby the PV panel was able to meet the load demand of 150Wh is 259 days.

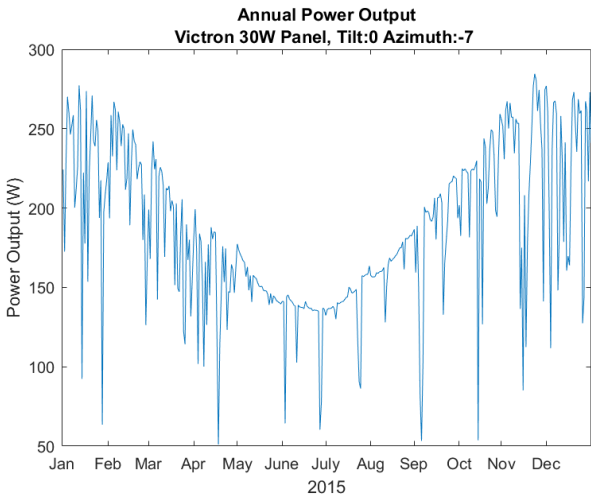


Figure 4.5: Daily PV Panel Output in 2015

The simulation shows that the PV panel does not produce sufficient energy for one third of the year. This is particularly visible during the winter months of June and July where the day is short and the night is long. For this reason, the size of the PV panel will be increased to 40W.

## 4.2 Battery

### 4.2.1 Selection of Battery Chemistry

Each battery chemistry has a different charging requirement and nominal voltage, and the selection of a battery chemistry will determine the features required in the charge controller. Lead acid, gel and lithium batteries are compared in Table 4.2 [19, 41]. The effective cost is an estimate of the actual cost of providing one kWh of energy considering the battery's lifetime and DoD.

Lithium-based batteries were selected as they require less maintenance than lead acid, and have a much longer lifetime. Between LiFePO<sub>4</sub> and other lithium batteries, LiFePO<sub>4</sub> does have a higher cost. However, this is offset by the large benefits in safety gained from selecting LiFePO<sub>4</sub>. Safety was a key decision driver because the project requires experiments and tests performed in the lab with circuits that are still in the development stage. Following this, LiFePO<sub>4</sub> batteries were selected.

	Lead Acid	Li-Ion	LiFePO4
Nominal Voltage	2V	3.7V	3.2V
Cycle Life	300-500	800-1000	2000-3000
Depth of Discharge	50%	80%	80-100%
Safety	High	Low	High
Estimated Effective Cost	£0.55/kWh	£0.33/kWh	N/A

Table 4.2: Comparisons of Battery Chemistries

#### 4.2.2 Series-Parallel Arrangement of Battery

A standard 18650 LiFePO4 battery comes with a nominal voltage of 3.2V and a capacity of 1.5Ah. The energy contained in each cell is 4.8Wh as calculated in Equation 4.1. To supply 150Wh, 32 battery cells are needed.

$$E = 3.2V * 1.5Ah = 4.8Wh \quad (4.1)$$

The selection of series parallel arrangement of the battery has implications on the charging time and current rating of the charge controller. The power rating of the charge controller is defined as:

$$P = V_{nom} * I_{charge} * t_{charge} \quad (4.2)$$

where  $V_{nom}$  is the nominal voltage of the battery,  $I_{charge}$  is the charging current of the charge controller and  $t_{charge}$  is the total charging time. If all the batteries were placed in parallel,  $V_{nom}$  would be 3.2V. Under a charging time of 5 hours, this would require 9.4A of charging current which in turn requires an expensive charge controller with high current ratings.

A quick search of available products on the market showed that many battery packs were sold in 12v arrangements. Besides that, the PV panel that was selected was marketed as a panel that is suitable for 12V systems. This suggested that 12V is a reasonable selection for the battery nominal voltage. As LiFePO4 comes with a nominal voltage of 12.8V, the most suitable arrangement would be 4 cells in series to provide 12.8V. Following this, there would be 8 cells in parallel, amounting to an amp-hour rating of 12Ah. Under a charging time of 5 hours, this would require 2.4A of charging current which is reasonable.

### 4.2.3 Battery Management System

As described in Section 2.4.4, a battery management system is needed to protect the battery from over-charge, over-discharge and over-current conditions. On top of this, the BMS should also perform cell balancing as the battery stack is a 4s arrangement.

There are battery packs available for purchase, and many of these are advertised as having an integrated BMS. However, there is little guarantee that they will be available in the exact 4S8P arrangement for users looking to implement this open-source design. Besides that, some battery packs only include over-charge and over-discharge protection but omit cell balancing. A more re-usable design should use standard battery cell sizes such as the 18650 cell that can easily be purchased from battery suppliers. For this reason, the implementation of a BMS that performs cell balancing was added to the scope of the project. A suitable 18650 LiFePO<sub>4</sub> cell from RS with a 1.5Ah capacity was identified for this design [22].

The specifications of the BMS should match the maximum allowable voltages and currents defined by the battery manufacturer. For the selected battery cell, the required BMS ratings are listed in Table 4.3 [22].

Specification	Value
Overcharge Voltage	3.65V
Overdischarge Voltage	2.5V
Overcurrent	3A
Cell balancing voltage	3.55V

Table 4.3: BMS Specifications

To develop the actual BMS circuit, a few options were considered. The first option was to buy a commercially designed BMS. A quick search of available products yielded very few options that could balance individual cells. Most products were designed for high-power applications like home solar systems, and the BMS would balance two 12V or 24V battery packs [42].

The next option was to select a suitable IC for a BMS circuit design. The potential ICs were identified and categorized (Figure 4.6). The ICs available are mainly split between the ones that only offer battery protection [43], and those that have cell balancing capability. Among the balancing ICs, some have integrated balancing FETs

while others can be used to control external balancing FETs. There is yet another sub-category: ICs requiring a host MCU and ICs that can be used without external controls [44, 45, 46]. Some standalone ICs come with protection and balancing thresholds factory programmed, while others can be programmed by the user (usually through EEPROM) [47, 48, 49]. Out of these options, the BQ7791506 was identified as the best option as it did not require any external MCU or FETs, being able to perform all the required functions with its internal features [50].

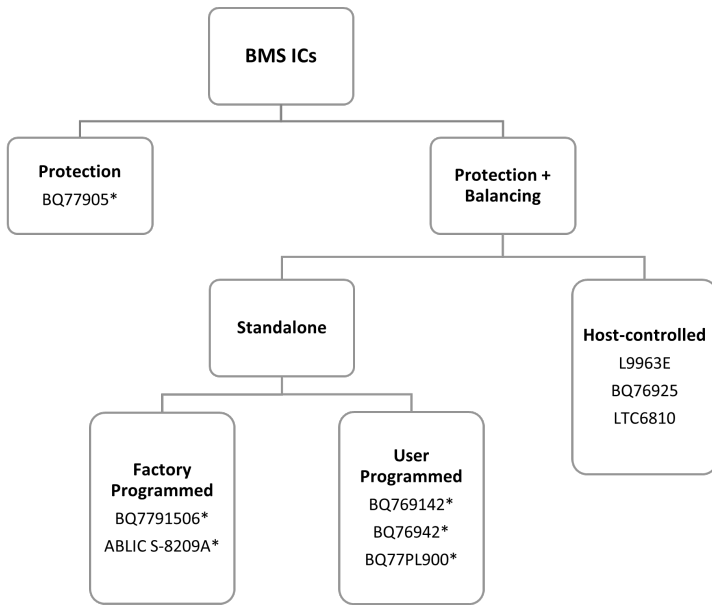


Figure 4.6: Categorisation of BMS ICs

However, the availability of many of the ICs including the BQ7791506 were very poor. All the ICs labelled with asterisks\* were out of stock on major retailers, with expected re-stock after the end of this project. The only ICs that were available were the ones that require a host MCU. This option would introduce a lot more complexity to the battery pack design, and might make the project overly focused on the batteries with insufficient time given to the design of the charge controller. For this reason, a fallback option was proposed for the BMS, with the host-controlled ICs left as an extension to the project if time permitted.

An open-source, discrete-component based BMS was designed by Dimitris Moniatis in "Design of a battery management system and a communication system for the open source wheelchair project" [51]. It was designed for a 6s Lithium Ion battery pack, with

protection and cell balancing features included. The design was well documented and included full schematics and code, so it will be easy to implement as a fallback version of the BMS. The voltage thresholds can easily be changed for a LiFePO<sub>4</sub> application.

### 4.3 Charge Controller

As discussed in the background section, the charge controller should perform the following functions:

- Step down the voltage from the solar panel voltage to the battery voltage
- Charge the lithium batteries using CC/CV charging
- Track the maximum power point of the solar panel

Besides implementing the three functions, the charge controller should be designed to work within the required voltage levels. The maximum input voltage of the PV panel must be more than the open circuit voltage of the PV panel which is not more than 25V for the considered range of solar panels. Similarly, the maximum output voltage of the charge controller should be larger than the maximum battery voltage. This is 14.4V for a 4s LiFePO<sub>4</sub> battery.

A review of materials on charge controller design determined that there are 3 ways to implement these functions. The first method is to work at systems-level by purchasing a readily available charge controller. There are products on the market that have been commercially designed, such as the Victron BlueEnergy MPPT Charge Controller range. While convenient, these come at a hefty cost at £153.28 [52].

The second method is a discrete component based charge controller. This would involve a Buck converter that can be adjusted to maintain the PV output voltage at the MPP and adjust the current. This would be controlled by a microcontroller that implements the MPPT algorithm and CC/CV charging [53, 54].

The third method is to use an IC that implements the Buck converter and/or the MPPT algorithm. There were a few ICs that were found to implement the necessary functions while meeting the required voltage ratings. This option was selected because using ICs that don't require programming make it very easy for users to implement this circuit. The potential ICs were compared in Table 4.4.

	LT3652	BQ24650	LT8490	BQ25798
Input Voltage Range	4.95V to 32V	5V to 28V	6V to 80V	3.6V to 24V
Output Voltage Range	3.3V to 14.4V	2.1V to 26V	1.3V to 80V	2.8V to 22V
Max Charging Current	2A	10A	>10A <sup>1</sup>	5A
CC/CV Charging	Yes	Yes	Yes	Yes
MPPT	Yes	Yes	Yes	Yes
Price	£7.37	£4.76	£17.01	£5.15

<sup>1</sup> Max charge current is dependant on the selection of external FETs

Table 4.4: Comparison of Charge Controller ICs

At the time of this project's design stage, semiconductor shortages were affecting the supply chain and some ICs were difficult to source. In particular, the BQ24650 and BQ25798 were not stocked by major suppliers such as RS, OneCall and Mouser. As such, the LT3652 was chosen even though it was more expensive than the aforementioned chips. However for future designs, it should be noted that these chips can also be used.

The only drawback of the LT3652 is the maximum charge current of 2A. This falls below the required charging current of 2.4A. To workaround this, two LT3652 charge controllers will be used in parallel, thus increasing the possible charge current to 4A.

Because the LT3652 performs MPPT, the effect of using two controllers in parallel on the same PV panel might yield ambiguous results. Hence, the PV panel will be split as well, using two 20W panels instead of one 40W panel. This necessity of using two PV panels and charge controllers in parallel presented the opportunity to split the whole system in two from the PV panel to the luminaire. The option of splitting the system was deemed a beneficial opportunity as it would reinforce the reliability of the PV streetlight. Besides that, since very little information was given about the lighting needs of the installation area, splitting the system has the added benefit of introducing modularity to the whole system. If the lighting is not enough, three strings in parallel can be used instead of two. Similarly, one string can be used if there is a need to cut costs and the area does not need that much light after all.

## 4.4 Luminaires

### LED Design

Among the technologies discussed in 2.5.2, LEDs are the most efficient and are thus chosen for the implementation of the luminaire. LEDs come in a few packages: Dual In-Line Package (DIP), Surface Mount Devices (SMD) and Chip on Board (COB).

COBs were chosen for the following two reasons:

- They have the highest lumens per watt capabilities, and this will help with the efficiency of the system
- Since each COB is able to emit a lot of light, they help to simplify the luminaire design. Instead of soldering around 50 SMD LEDs onto a board, a COB based design would only need 5-10 devices produce the same amount of light.

COB LEDs come in various voltages, current ratings and luminous flux. The most common COB devices have voltages of 3V or 12V, and the brightness depends on the current that is passed through the device. Since the batteries are arranged in a 12.8V combination, the 12V COB devices were a possible choice. However, some consideration was given to the LED driver device (further discussed in Section 4.4). Many of these devices are DC-DC converters that help to regulate the current input to the LED. If a buck converter is used, it might require a minimum dropout voltage (ie. the output voltage must be lower than the input voltage by a certain margin). Given these considerations, the 3V COB devices were selected and will be arranged in series.

Following the decision to split the system (Section 4.3, the LEDs will also be arranged in two parallel strings. This adds up to a total of 6 LEDs for the luminaire. The target luminous flux of 2100lm is divided by the 6 LEDs, yielding a requirement of 350 lm per LED.

The XM-L2 series by Cree was selected for this application as it meets all the requirements. In particular, the XMLBWT-00-0000-0000U2051 was selected. It has a nominal voltage of 3.3V and can be driven with currents of up to 3A. The luminous flux at 300 lm @ 700mA and 412 lm @ 1000mA. Driving it at approximately 850mA would produce the target 350 lm per COB. Operating the LED at a current lower than its maximum also reduces the concerns about thermal dissipation. [55]

## Power Rating of LED

When driven at 850mA, the LED has a nominal voltage of 3V. The total power requirements of the LED is:

$$P = 3V * 0.85A * 6 = 15.3W \quad (4.3)$$

This is lower than the initial estimate of 21W because the chosen LEDs have a higher lm/w rating. Based on this power rating and a battery capacity of 150Wh, the streetlight would be able to operate at full brightness for 9-10 hours. This exceeds the initial target of 6 hours at full brightness.

## LED Driver

The LED driver should be rated for 12V systems, and must supply an output current of 800mA. Similar to the charge controller and battery management system, it can also be implemented via three levels of abstraction: a ready-made design, IC-based or discrete component-based.

The IC-based design was first considered because it is a good trade-off between cost and complexity. Besides that, LEDs are very generic circuits, so many options for ICs can be found on the market. A search of the available LED drivers identified the LM3405A by Texas Instruments to be suitable for this design. It is a buck LED driver with an input voltage range of 5V - 22V, and an output current of 1A. The circuit design for this device is also relatively simple. [56]

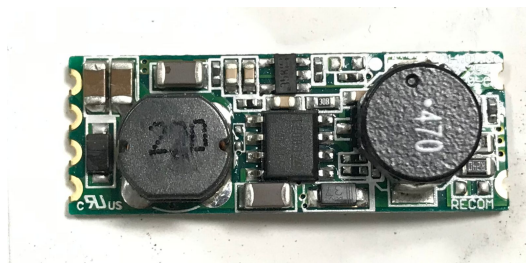


Figure 4.7: RECOM LED Driver

With the limited time of the project, a fallback option was also proposed for the LED driver. The Recom RCD-24-1.00/PL/A was identified for this. It is a step down converter with a maximum output current of 1A. [57] This circuit board was first purchased

and used for the system, and the IC-based design was categorised as an extension to this project.

### Brightness Control

The final section that needs to be designed is the control of the luminaire. Earlier in Section 3.1, a scheme for increasing the runtime of the streetlight was proposed. The luminaire will be reduced to 50% brightness when there is no traffic near the streetlight. When there are pedestrians, a PIR sensor will detect the motion and trigger the brightness to be increased to 100%. The streetlight will remain in this full brightness state for 5 minutes before switching back to 50% brightness. Besides this, the LED also needs to be switched on at dawn and switched off at dusk. An LDR will be used to detect the ambient light levels.

The Recom RCD-24-1.00/PL/A LED driver comes with PWM dimming control, analogue dimming control and on/off control accessible via a pin [57]. This pin can be controlled by a microcontroller that receives stimuli from the PIR and LDR sensors. The Arduino Nano used to control the BMS can be used to implement the LED brightness controls also.

## 4.5 Revised System Sizing

The key decisions that were made during the analysis and design stage are summarised as follows:

- Increase the PV panel from 30W to 40W
- Split the system into two identical parallel strings

The full revised system is illustrated in Figure 4.8, and is labelled with the voltage levels, current flows and power ratings for each subsystem.

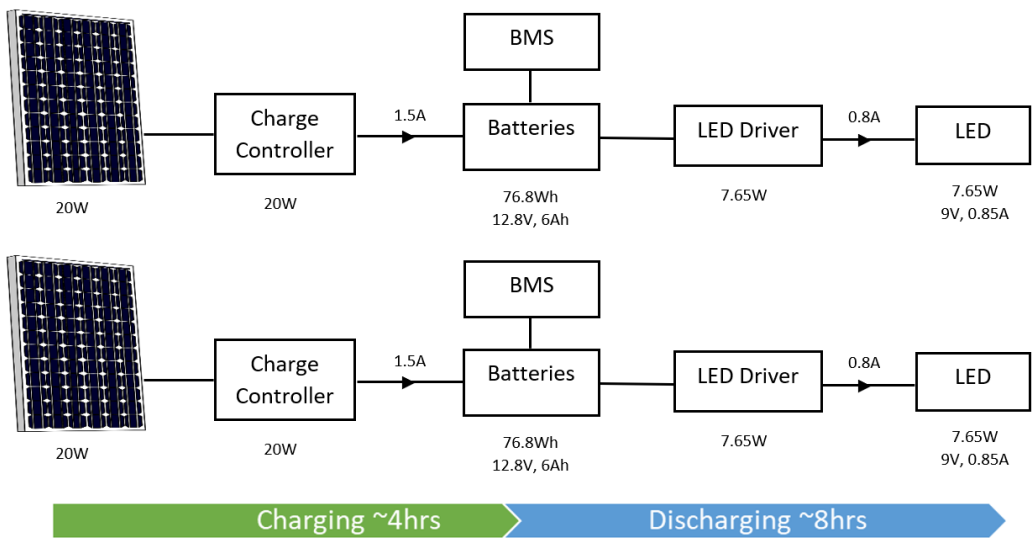


Figure 4.8: Full System Level Design

# Chapter 5

## Subsystem Implementation

### 5.1 Charge Controller

#### 5.1.1 Circuit Design

The LT3652 is the core of the charge controller circuit. Figure 5.1 shows the complete circuit that was designed based on guidelines and reference designs from the LT3652 datasheet [58]. J1 is the input for the PV panel, and J3 is the connection to the battery. The circuit can be grouped into 3 main sections: the DC-DC converter (plus switch driver), input programming section, and output programming section.

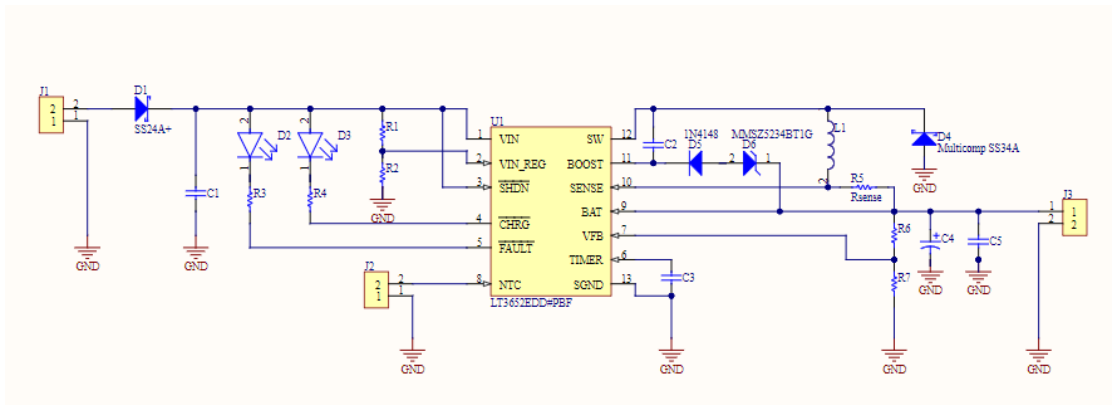


Figure 5.1: Charge Controller Circuit Schematic

The IC contains an internal BJT switch, with its collector connected to the  $V_{IN}$  pin and the emitter connected to the SW pin. The external inductor L1 and diode D4 are connected to the switch via SW to complete the Buck converter topology. The IC has internal logic that controls the switch after comparing the output current with the

battery voltage. The bootstrapping circuit consists of capacitor C2, diode D5 and D6 connected to the BOOST pin. This circuit uses part of the battery voltage to help drive the switch and ensure it is in saturation. [58]

The main part of the input section is the potential divider R1/R2 connected between the  $V_{IN}$ ,  $V_{IN\_REG}$  and GND pins. These resistors are sized such that  $V_{MPP}$  at the  $V_{IN}$  pin corresponds to 2.7V at the  $V_{IN\_REG}$  pin. The IC performs pseudo-MPPT by maintaining the PV panel voltage at the programmed  $V_{MPP}$  (ie. 2.7V at  $V_{IN\_REG}$ ). If the input voltage drops below  $V_{MPP}$ , the IC reduces the maximum output current, which in turn reduces the current drawn from the PV panel. This brings the operating point past the elbow of the PV curve and increases the voltage to be greater than or equal to  $V_{MPP}$ . [58]

The other components in the input section perform the following functions. Diode D1 is a zener diode that prevents the current from flowing in the reverse direction when the solar panel is not producing electricity, and capacitor C1 decouples the input from the chip. The LEDs connected to the CHRG and FAULT pins serve as indicators to the status of the IC, and resistors R3, R4 limit the current through the LEDs. [58]

At the output section, resistor divider R6, R8 set the maximum battery float voltage. This voltage is the point where the charger switches from constant current to constant voltage mode. These resistors are sized such that the maximum  $V_{BATT}$  corresponds to 3.3V at the  $V_{FB}$  pin. The resistor  $R_{sense}$  programmes the maximum charging current of the circuit. C4 and C5 are an electrolytic and ceramic capacitor respectively that serves as bypass capacitors at the output of the charger. [58]

At this stage of the design, the component sizes and minimum ratings were calculated but the exact parts were not selected yet. The charge controller's target specifications are  $V_{in,max} = 23V$ ,  $V_{batt,max} = 14.4V$  and  $I_{charge,max} = 1.5A$ . The ratings of each component was designed with slightly higher specifications in mind for enhanced reliability and increased tolerance. The components are all rated for at least 30V at the input, 14.4V at the output, and 2A of charging current. The LT3652 datasheet contains all the exact equations for component sizing [58]. Following the guidelines, the minimum sizes and ratings were calculated and summarised in Table 5.1

Identifier	Value	Minimum Ratings
L1	15uH	$I_{sat} > 2.6A$ , $I_{RMS} > 2A$ , $Volt-second > 8$
D1	Schottky	$V_{rev} > 30V$ , $I_{diode} > 1.2A$
D2, D3	LED	-
D4	Schottky	$V_{rev} > 30V$ , $I_{diode} > 1.3A$
D5	Silicon	$V_{rev} > 30V$ , $I_{diode} > 0.1A$
D6	Zener	$V_f > 6V$ , $I_{diode} > 0.1A$
C1	$10\mu F$	30V, 1A
C2	$1\mu F$	-
C3	$100\mu F$	Electrolytic, 14.4V
C4	$10\mu F$	Ceramic, 14.4V
C5	$0.68\mu F$	-

Table 5.1: Minimum component values and ratings as advised by LT3652 datasheet

Inductor L1 is designed to keep the output ripple to within  $0.3I_{charge}$ . The current rating of diode D1 isn't specified, but should be larger than the short circuit current of the PV panel. The forward voltage of Zener diode D6 also is not specified, but must be larger than  $V_{float} - 8.4V$ . The values of the resistors are as labelled in Figure 5.1. For 1.5A of charging current,  $R_{sense}$  should be a  $0.068\Omega$  precision resistor.

### 5.1.2 LTSpice Simulation

An LTSpice model of the LT3652 and its reference design is available on the product page on Analog Device's website [3]. This helps to verify the selection of components and the functions of the IC before implementing the circuit on hardware.

Figure 5.2 shows the spice schematic with the component values edited according to the component sizing performed in Section 5.1.1. A PV panel model was also designed for this simulation, and the details are included in Appendix A. The battery was represented by a 10mF capacitor. It has a much smaller capacity than the expected battery so that the simulation time can be reduced. The voltage of the capacitor was initialised to be lower than the precondition threshold. This represents a very low battery SoC, under which condition the battery needs to be trickle charged. The voltage level of the capacitor gradually increases during the simulation as charge is added. Eventually, it enters into constant current and subsequently constant voltage charging.

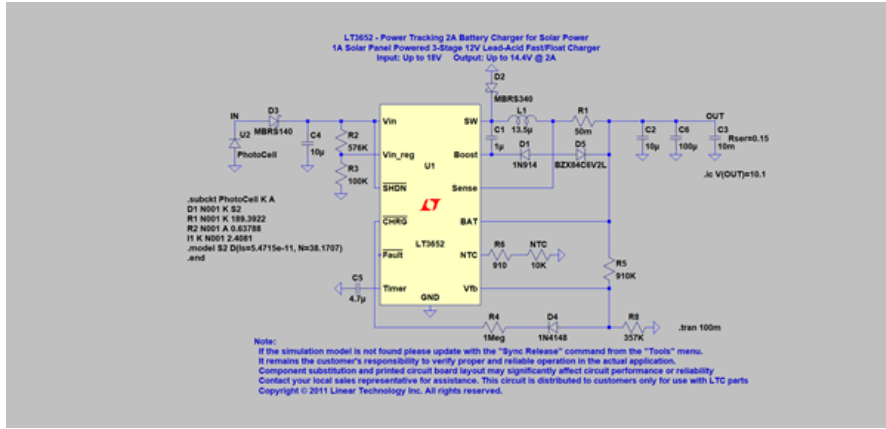


Figure 5.2: Charge Controller LTSpice Circuit [3]

Figure 5.3 shows the full simulation of the circuit's behaviour during the three stages of charging. The voltage,  $V_{PV}$  and current,  $I_{PV}$  of the PV panel are shown in red and teal respectively. The charging current,  $I_{charge}$  is shown in blue, while the battery voltage,  $V_{bat}$  is shown in green. The graph shows the three charging modes (trickle charge, constant current, constant voltage).

In the precondition stage, the battery voltage is very low and the charging current is kept low. Concurrently, the LT3652 controls the PV voltage and current to draw low amounts of power for the charging process, and operates very near the open circuit voltage,  $V_{OC}$ . The behaviour in this region was simulated to verify its performance. In the actual operation, the BMS will prevent the voltage of the battery from reaching such low levels that it requires preconditioning.

As  $V_{bat}$  reaches 10.25V, it enters constant current mode where the charge controller outputs the maximum charging current. The battery voltage rises linearly as it is charged at a constant current. The LT3652 decreases the PV voltage from the open circuit voltage to draw more current. Throughout the constant current stage, the MPPT gradually increases the power drawn from the PV panel, as seen by the linear slope of  $V_{PV}$  and  $I_{PV}$ . This can be credited to the increasing battery voltage that leads to an increasing power requirement.

Once the battery voltage reaches the full float voltage, the charger enters constant voltage mode. The charging current is decreased to maintain a constant battery voltage.  $V_{PV}$  is increased past  $V_{MPP}$  to decrease the current and thus decrease power draw from

the PV panel.

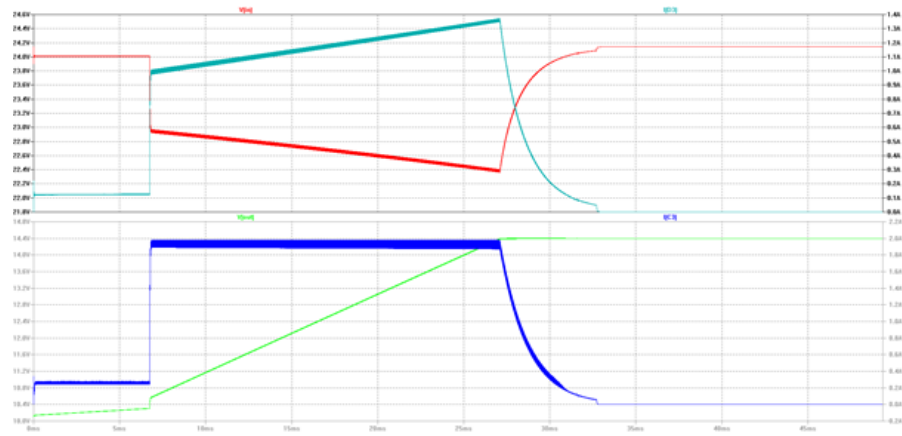


Figure 5.3: Simulation of Charge Controller

### 5.1.3 Evaluation Board

For the evaluation board, two alternatives were considered instead of the DC1568A by Analog Devices because the £95 price was rather expensive for the low component count. The two other options were the Sparkfun Sunny-Buddy board [59] and an open source PCB design [60] (Figure 5.4. Both options feature the LT3652 chip and can be used to validate its basic charging functions.

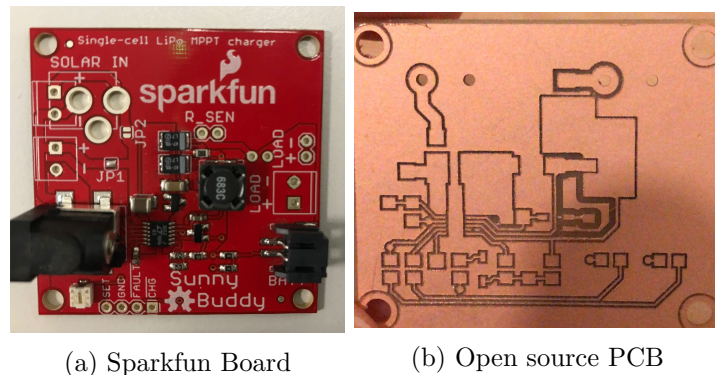


Figure 5.4: Options for evaluating LT3652

The open source PCB was milled in the lab, but was not fully assembled because two of its pads became detached from the board during soldering. However, the components

had already been purchased following the open source design’s bill of materials, and the ratings of the diodes were found to meet the specifications in Table 5.1. Because of this, the same diodes were eventually used in the final circuit design (Figure 5.1) and credit for their selection is given to the open source design [60].

Following this, the Sparkfun board was purchased and used to validate the IC. The board comes assembled with components designed for a 3.7V LiPo battery and 450mA of charging current. The board was tested using the setup in Figure 6.1. The results in Figure 5.5 show the results of this test, with the charging current confirmed to operate according to CC/CV charging.

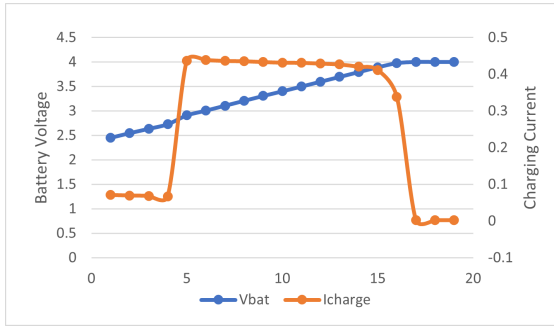


Figure 5.5: Evaluation of LT3652 using Sparkfun Board

Having validated the physical IC’s performance, the next step was to select the actual components for the design. As mentioned earlier, the diodes from [60] as they were already on hand. The other components were selected according to the values and minimum ratings in Table 5.1, and are listed in the bill of materials in Appendix B.

#### 5.1.4 PCB Design

Since the objective of this project is to release the files as open source, CircuitMaker was selected as the PCB design software over commercial products like Altium Designer. CircuitMaker is a free software and has good support for open source projects. Project files can easily be forked from the public repository and edited if the user prefers slight changes, for example, in the component packages. Furthermore, CircuitMaker files can be directly opened and edited in Altium Designer, whereas the process to import files from Altium Designer to CircuitMaker is complicated.

The LT3652 datasheet emphasizes the need to keep the switching current away from the

main power paths. This is because interference can result in reduced performance of the chip. The guidelines on component placement were followed very closely so that the switching current has a well defined path to ground. Large ground pours are also used to provide thermal relief for the IC, and effective grounding for all the signals. The result of this design process is shown in Figure 5.6. A standard 2 layer FR4 board was selected for this design. A ground pour was done on both layers of the PCB. The bottom layer also routes the power signals between the IC and the battery, utilising the ground plane to shield it. The main power paths were routed with an increased width of 20mil. The board was assembled as shown in Figure 5.7.

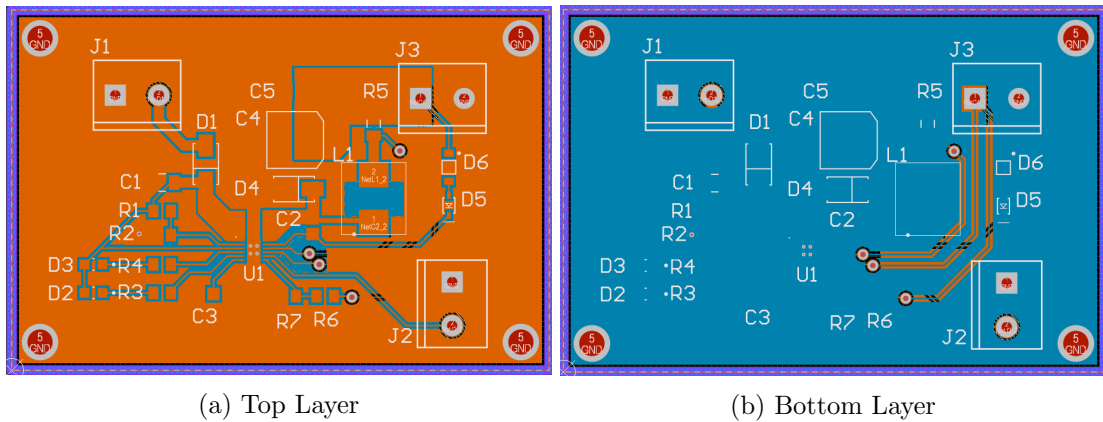


Figure 5.6: Charge Controller PCB

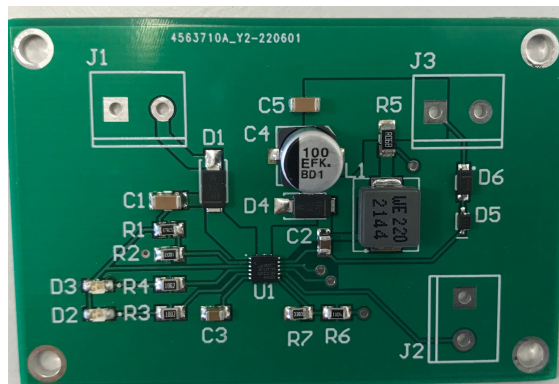


Figure 5.7: Assembled Charge Controller Board

## 5.2 Battery Management System

As per Section 4.2, an open-sourced BMS will be re-purposed for this project. The original design used an STM32 MCU and contained many auxiliary functions for communication, which was not needed for this project. For this reason, a PCB was re-designed to only include the voltage reading and cell balancing circuit for 4 cells. The schematic created for the PCB design is shown in Figure 5.8. Full credit is given to the original author for the design and implementation, as well as the explanations for the function of each component in the circuit [51].

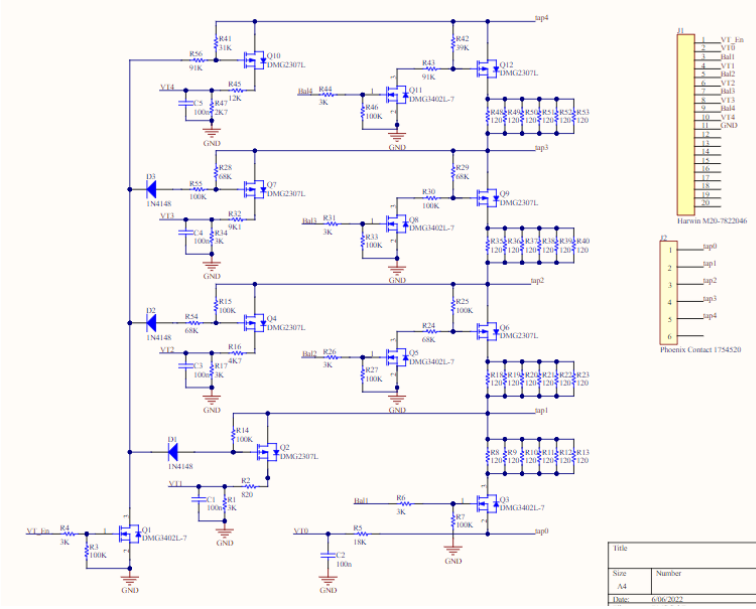


Figure 5.8: Cell Balancing Circuit

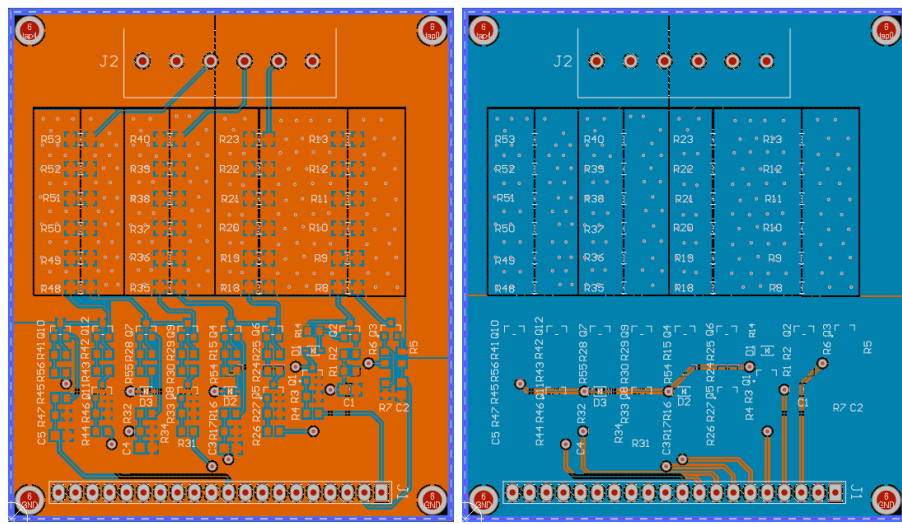
On the voltage reading side, transistors Q2, Q4, Q7 and Q10 are enabled when voltage readings are taken. When no readings are taken, these transistors are switched off to reduce the power consumption of this balancing circuit. In the original design, there was a problem with the MOSFETs at the 4th, 5th and 6th branch leaking current even when they are supposed to be off. This same problem was anticipated for Q10. The suggestion given in the report was to select a PMOS with a larger  $V_{DS}$  rating, and this advice was followed. Resistor dividers R45/R47, R32/R34, R16/R17 and R2/R1 bring the voltage readings down to the acceptable range of the microcontroller ADC pins. [51]

For the cell balancing circuit, transistors Q3, Q6, Q9, Q12 are the main switching MOS-

FETs that control the switching on/off of the balancing current while Q5, Q8 and Q11 shift their gate levels down. When they are asserted, the current from the cells flow through from drain to source and are bled through the network of resistors. Again following the advice from the original design, 6  $120\omega$  resistors were used to provide a power rating of 1.5W. The power rating requirements of this circuit are lower than the original design, since LiFePO<sub>4</sub> cells have a lower nominal voltage than other Li-Ion cells. The original selection of 6 resistors was maintained as it would provide good headroom for the power dissipation. [51]

The selection of MOSFETs proposed in the original version were out of stock with long lead times reported, so new MOSFETs were selected. As mentioned before, the PMOS needs to have a large  $V_{DS}$  rating to prevent the leakage currents. A  $V_{DS}$  of 30V is selected as it is more than double of the 14.4V maximum voltage expected in this circuit. The currents through the switching MOSFETs are in the mA range, so an  $I_{DS}$  rating of 3A is targeted. Following these target specifications, the DMG2307L and DMG3402L-7 were selected as the PMOS and NMOS respectively. The DMG2307L has a voltage rating of 30V and current rating of 4.6A, while the DMG3402L-7 has a voltage rating of 30V and current rating of 4A.

A 2 layer PCB was designed with the layout following guidelines in [51]. One of the main issues highlighted in [51] was the need for good heat dissipation, as the resistors were reaching 120°C. The resistor bank at the top of the PCB was spaced out even further and polygon pours were used to connect the same nets together. The repetitions in the circuit designed allowed for a neater arrangement of components on the board. The components on the bottom half of the PCB were manually placed, but were autorouted to help with managing the many connections. Finally, some manual routing was done to tidy the board where possible. The board was assembled as shown in Figure 5.10.



(a) Top Layer

(b) Bottom Layer

Figure 5.9: Cell Balancing PCB

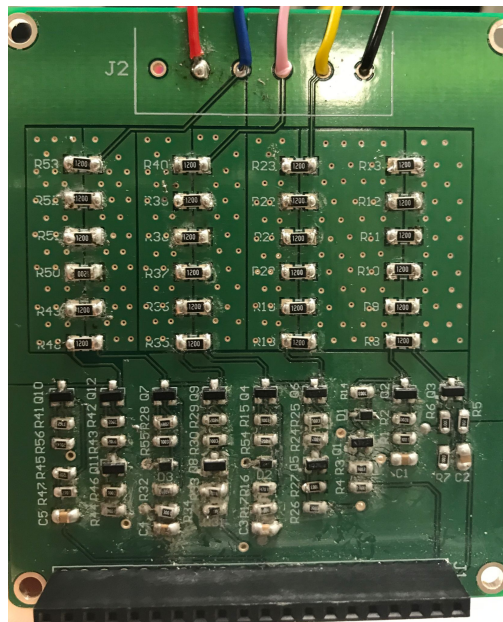


Figure 5.10: Assembled BMS

An Arduino Nano was used to control the BMS. The voltage reading and cell balancing algorithm was adapted from the original design from STM32-compatible code to Arduino compatible code [51].

### 5.3 Luminaires

The luminaire consists of a string of 3 surface mount COB LEDs. To connect them together, a PCB was designed with spacing between each LED so that it can directly be mounted in the streetlight. Having only 3 components on the board simplifies the layout and PCB design. However, the PCB requires good heat dissipation as COB LEDs dissipate a lot of heat. The PCB thermal guidelines provided in the Cree XM-L2 design guide were followed [61]. Thermal vias were added near the LED solder pads, and a large copper pour was made on the top and bottom layer for heat dissipation. Besides that, an aluminium base is used instead of the regular FR-4 material since aluminium provides better heat dissipation. The resulting PCB design is shown in Figure 5.11.

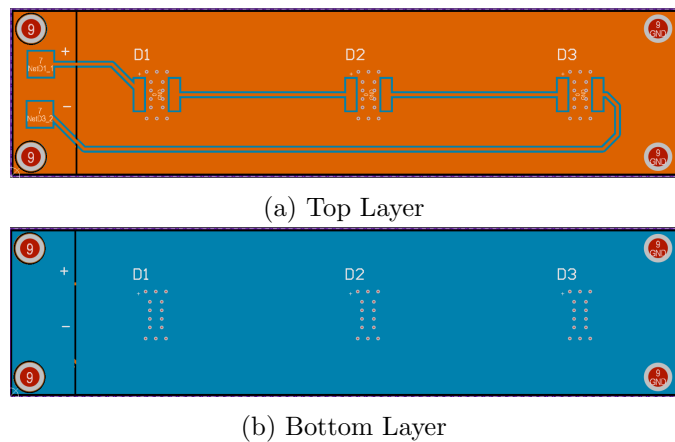


Figure 5.11: LED PCB

# Chapter 6

## Testing

### 6.1 Charge Controller

#### 6.1.1 Setup

Power supplies are used to emulate the PV panel and battery pack at the charge controller's input and output respectively. The PSU is used in place of the battery to ensure a safe testing environment while the circuit's behaviour under different operating conditions is being validated. Using a PSU to emulate the PV panel allows for greater control of the testing environment as different sunlight conditions can be artificially setup and maintained while the data is being recorded.

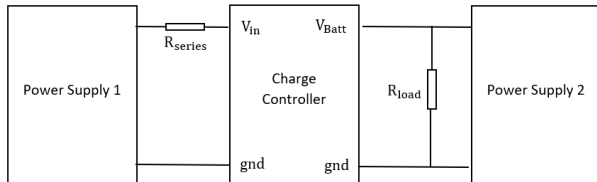


Figure 6.1: Setup of controlled environment for testing charge controller

Figure 6.1 shows a block diagram of the test environment setup following the advice from the LT3652 evaluation board user guide [62]. Power Supply 1 (PS1) emulates the PV panel, and its voltage and current limit should be set to the PV panel's  $V_{OC}$  and  $I_{SC}$  respectively. The voltage dropped across  $R_{series}$  varies with the current drawn from PS1, and this allows the MPPT function of the circuit to be tested. The value of  $R_{series}$

can be changed to emulate different irradiance conditions.

$$R_{series} = \frac{V_{OC} - V_{MPP}}{I_{MPP}} \quad (6.1)$$

The battery emulator consists of Power Supply 2 in parallel  $R_{load}$ . The power supply sets the battery voltage, and the  $R_{load}$  sinks the current from the charge controller. The value of  $R_{load}$  should be selected such that the current flowing through it is larger than the maximum charge current [63]. If the output from the charger decreases, the power supply provides the deficit current to  $R_{load}$ . When there is no current from the charger, the power supply sources the full current through  $R_{load}$ . The current drawn by  $R_{load}$  is the power supply voltage divided by the resistance of  $R_{load}$ .

$$I_{sink} = \frac{V_{PS2}}{R_{load}} \quad (6.2)$$

The minimum current through the resistor,  $I_{sink}$ , corresponds to the minimum  $V_{PS2}$  which is 10.5V (Section 5.1.2). To sink 1.5A at 10.5V, the value of the resistor should be:

$$R_{load} = \frac{10.5V}{1.5A} = 7\Omega \quad (6.3)$$

The power rating of the resistor needs to be larger than the power flowing through it at maximum voltage and current conditions:

$$P = \frac{14.4V^2}{7\Omega} = 29.6W \quad (6.4)$$

Figure 6.2 shows the implementation of the test setup in the lab using two bench power supplies and a variable resistor that was selected due to its large power rating.

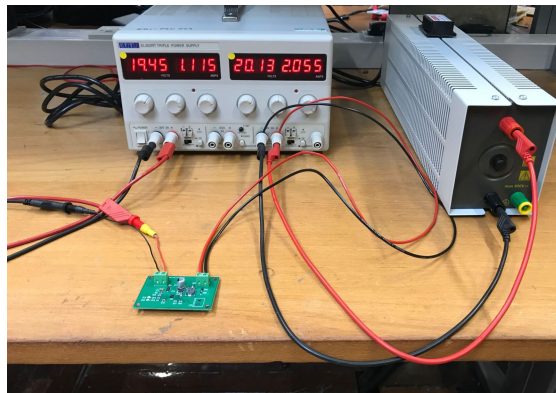


Figure 6.2: Implementation of charge controller testing environment

### 6.1.2 Validation of CC/CV Charging

To begin, the basic CC/CV charging function of the circuit was validated. For this, the series resistor in Figure 6.1 was omitted as the MPPT function was not being studied yet. The voltage and current limit of PS1 was set at 19.5V and 1.1A respectively.

The battery emulator was first set to 10.5V and incremented in steps of 250mV to 14V. The battery voltage was further incremented from 14V to 14.4V in steps of 50mV to as this is the range where the charger is expected to switch from CC to CV mode. The charging current and PV output current at each battery voltage step was recorded. The charging current and battery voltage were plotted in Figure 6.3. The graph shows the two modes of charging - below 14.3V, the charging current is relatively constant, before tapering off very quickly once the battery reaches 14.3V.

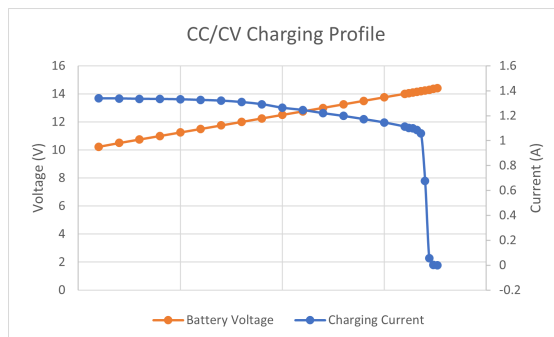


Figure 6.3: Graph of CC/CV charging at peak power conditions

The graph shows that the maximum charging current is 1.4A instead of the 1.5A that it was designed for. This could be due to parasitic resistances in series with the current programming resistor.  $R_{sense}$  is a  $0.068\Omega$  resistor, so slight deviations in the actual resistance or resistance from additional sources like the PCB tracks can cause a shift in the maximum charging current. For future designs, a high precision resistor should be chosen for  $R_{sense}$  and the width of the PCB track should be increased.

### 6.1.3 Validation of MPPT

To understand how the charge controller controls  $V_{PV}$  and  $I_{PV}$ , its behaviour was studied under two operating conditions. The test environment was setup as shown in Figure 6.2, with  $R_{series}$  included in this experiment. Two different values of  $R_{series}$  were used to

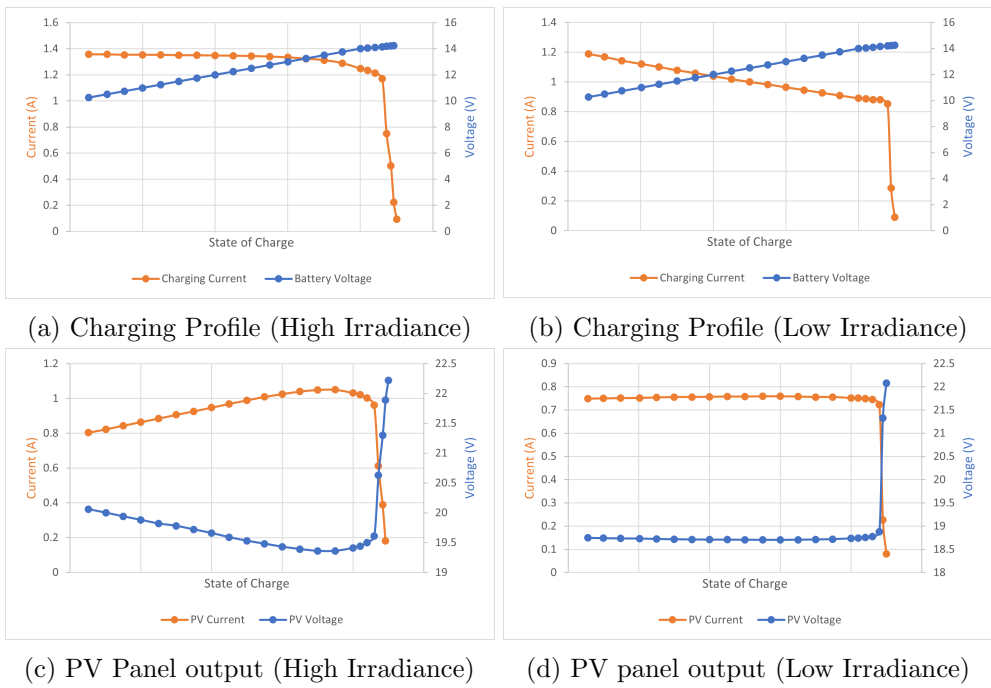


Figure 6.4: Charge controller setting the operating point of the PV panel

simulate low irradiance and high irradiance conditions.

The 4 graphs presented in Figure 6.4 illustrate the circuit controlling the operating point of the PV panel. When there is sufficient light, the power produced by the PV panel at MPP is more than the power requirements of the charger. Under this condition, the charge current is maintained at its maximum output for the duration of the constant current charging period (Figure 6.4a). The charge controller does not need to track the MPP since there is sufficient power even at lower operating points on the Pv panel curve. Figure 6.4c shows the charge controller setting  $V_{PV}$  and  $I_{PV}$  at a lower operating point at the beginning of the charging period. As the battery's voltage gradually increases with the state of charge, the power requirements also increase. The charge controller responds to this by changing the operating point of the PV panel to draw more power. The linear slope in Figure 6.4c is representative of the PV panel operating point shifting closer to the maximum power point. When the charger enters constant voltage mode, the power point is shifted away from the elbow of the solar panel's curve because the power requirements have reduced.

During low light conditions, the power from the PV panel is not sufficient to charge the

battery at the maximum charging current. The charge controller reduces the charging current in response to the limited input power, as seen by the charging current capped at 1.2A in Figure 6.4b. As the battery voltage increases, the charging current reduces further because it cannot draw extra power from the PV panel. Figure 6.4d confirms that the PV panel is at its maximum power point throughout the constant current period as the voltage and current are being held constant.

Figure 6.4d demonstrates the charge controller's ability to maintain the maximum power point for a given level of irradiance. In practice, the irradiance will be shifting throughout the day so the charge controller's response to varying irradiance also needs to be tested. This was emulated using the same test setup in Figure 6.1, and sweeping the value of  $R_{series}$  to represent the changing irradiance. The results of this test are seen in Figure 6.5. Estimates of the PV panel I-V curve were added to illustrate the charger tracking the MPP. The MPPT stops when the PV input power is larger than the power requirements for charging the battery.

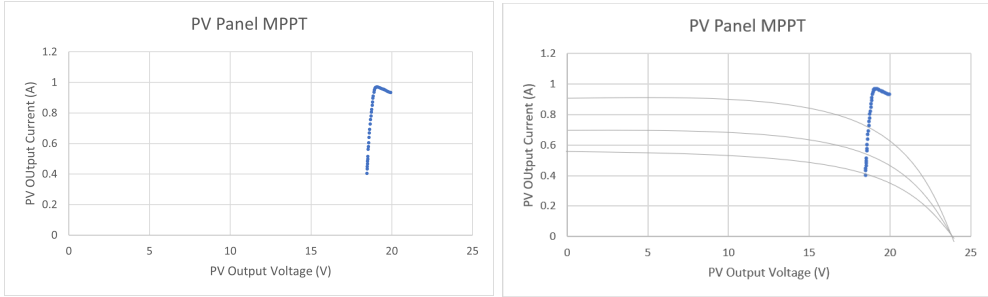


Figure 6.5: Charge controller MPPT under varying irradiance

#### 6.1.4 Efficiency

The charge controller's efficiency was measured across the range of operating battery voltages and plotted in Figure 6.6. The converter displays up to 88% efficiency in the given range, and this matches the expected efficiency from the datasheet [58].

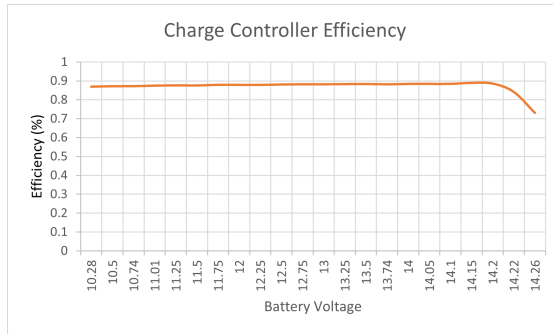


Figure 6.6: Charge controller efficiency across different battery voltages

## 6.2 Battery Management System

### 6.2.1 Setup

In practice, the BMS should be connected with batteries between each tap. However since the usage of batteries during testing presents a large safety risk, the circuit is first validated using a resistor ladder (Figure 6.7) to mimic the voltages of each cell. The resistors are connected in a 4-series arrangement to represent the 4 cells in series. When the power supply is connected between the two pins at the top of the circuit board, the voltage will be split evenly between the 4 resistors in series. The value of the resistors is selected to maximise the current flowing through the resistor divider while keeping the power rating requirements within a reasonable range.

The resistor ladder should have 100mA during the lowest current conditions of  $\text{Bat}+ = 10\text{V}$ . The total resistance required to achieve this is  $100\Omega$ . With this resistance, the current flow through each 'cell' during the maximum  $\text{Bat}+$  voltage of 14.4V is 144mA. Under this condition, the minimum power rating of each series resistor is

$$P = \frac{3.6^2}{25} = 0.5184W \quad (6.5)$$

An arrangement of 5 0.125W resistors in parallel would increase the power rating to 0.625W which meets the requirements. There were no  $125\Omega$  resistors available, so  $\Omega$  resistors were chosen instead. This results in a minimum voltage of 104mA and power rating requirement of 0.54W, which meets all the targets.

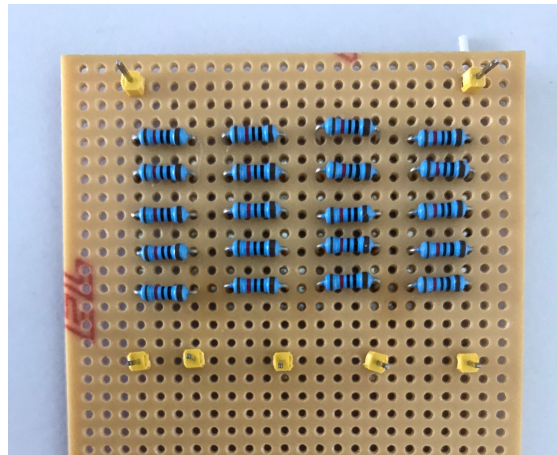


Figure 6.7: Resistor ladder used to mimic cell voltages

The resistor ladder was connected to the power supply and the battery pins of the BMS PCB. The microcontroller was then connected to the logic pins of the BMS PCB as shown in Figure 6.8.

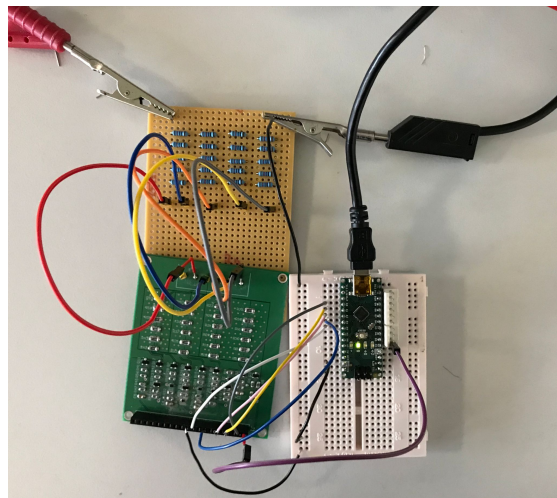


Figure 6.8: Test setup of BMS with resistor ladder to emulate the battery voltages

### 6.2.2 Voltage Measurement Circuit

The first task was to check that the voltages at the VT0-VT4 pins of the BMS were correctly divided according to the resistor dividers. For this, the microcontroller was first detached and the voltages at the said pins were probed using a multimeter. During the initial testing, it was found that the voltages at each node was different from the

expected voltages. Debugging this lead to the finding that this was because the ground of the BMS was left floating. Though there is no explicit ground-VT0 connection in the BMS schematic, it was found that this connection is necessary and did fix the problem. The next problem that was encountered was due to an oversight in the PCB design process, with the PMOS being connected in the wrong orientation. This error lead to leakage currents flowing through the PMOS when they were supposed to be switched off.

After the two problems were fixed, the BMS was tested again. This time, the voltage measured at the VT pins of the BMS were the expected voltages and they fell within the acceptable range of the microcontroller. An additional test was conducted to check whether the leakage currents reported in the original design were fixed by the suggestion given in the report to select a PMOS with a larger  $V_{DS}$  rating [51]. Indeed, the advice was accurate and PMOS Q10 no longer leaked current when switched off. The entire circuit was found to have no leakage currents when all the MOSFETs were switched off.

The next task was to map the ADC values read by the microcontroller with the actual voltages at each cell as measured by a multimeter. The methodology for this mapping was also taken from [51]. The voltage of the power supply was swept from 9V to 15V, and the ADC values at each pin was recorded. The multimeter was used to measure the voltage at each cell. Finally, the actual voltage was plotted against the ADC readings and the Microsoft Excel lines of best fit was found (Figure 6.9).

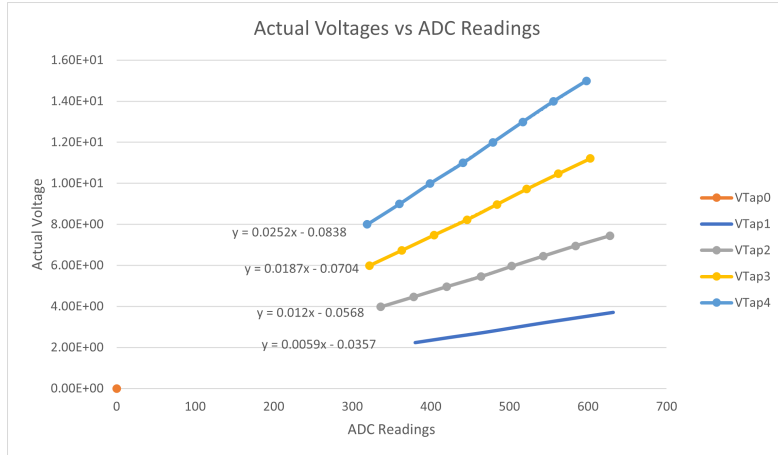


Figure 6.9: Graph of actual cell voltage plotted against ADC reading of microcontroller for calibration of voltage reading circuit

The equations of lines of best fit were inputted into the voltage reading code. This was validated by performing another voltage sweep of the battery voltage, and recording the voltage calculated by the microcontroller. The actual cell voltages were once again measured using a multimeter, and the results are plotted in the same graph to check for any discrepancies in the microcontroller's voltage reading capability. Figure 6.10 shows the microcontroller's ability to read the voltages accurately. The large error seen while measuring the voltage at Cell 1 is due to this voltage being too low, and the ADC is not sensitive enough at this range. However, the lowest expected voltage at Cell 1 is 2.5V, at which point the graph shows good correlation between the multimeter and microcontroller readings.

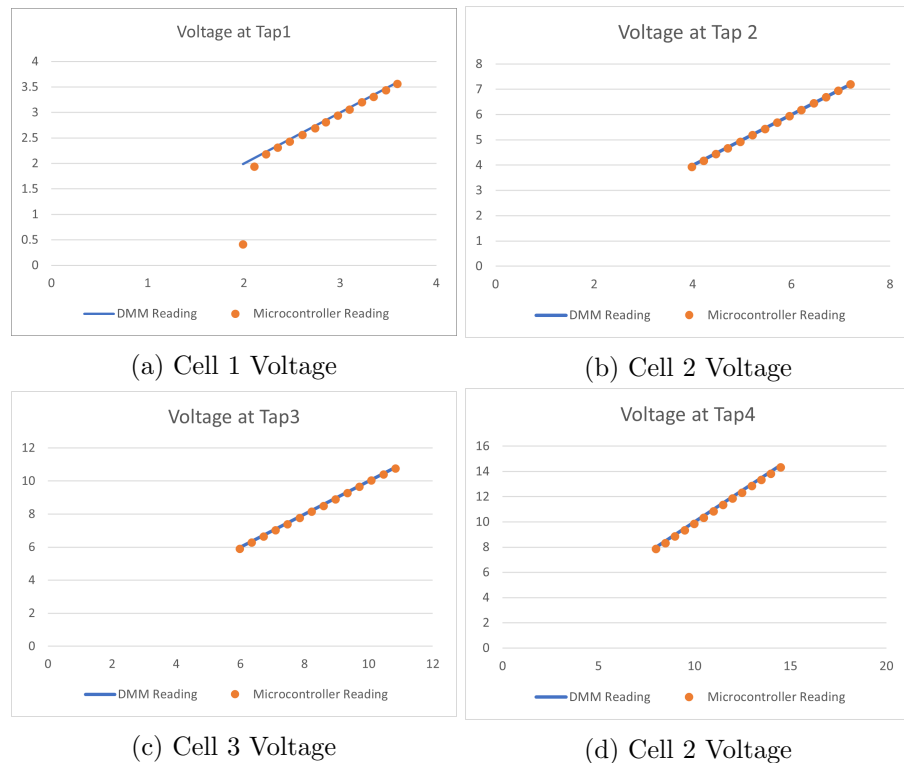


Figure 6.10: Graph of cell voltages read by multimeter and microcontroller

### 6.2.3 Cell Balancing Circuit

The first task in validating the cell balancing circuit is checking that the MOSFETs Q3, Q6, Q9 and Q12 switch on when asserted and measuring the current flow through them. A 'high' signal was applied at each of the Bal1-Bal4 pins, and the total battery voltage was swept from 13.9V to 14.5V to determine the balancing current during this range of

voltage conditions. This is the voltage range where the balancing gets triggered as it is near to the max float voltage of the battery cells (3.6V each). To measure the current, the connection between the resistor ladder and BMS PCB is broken and an ammeter is connected in between the pins. Figure 6.11 displays the results of this experiment, and the currents are found to be within the range of 89mA to 94mA.

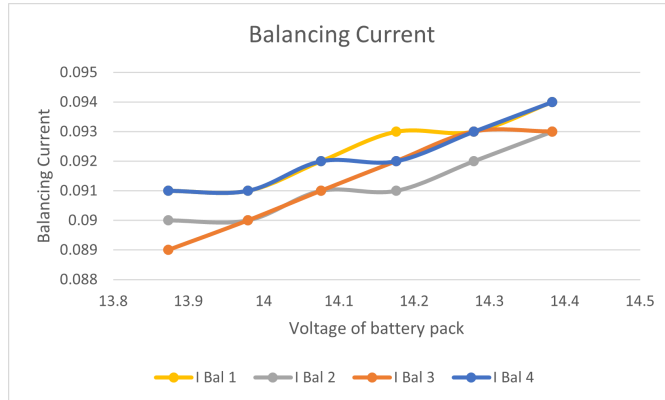


Figure 6.11: Graph of balancing current at each cell for a range of battery voltages

Next, the cell balancing algorithm was tested by fully connecting the microcontroller pins to the BMS logic pins. To emulate one cell having a lower voltage than the rest, an extra resistor was connected in parallel with one of the 'cells'. This results in a lower resistance across this branch, and less voltage being dropped across it in the resistor divider. The BMS PCB was viewed using an infrared camera to measure the temperature of the bleeding resistors during this operation. Figure 6.12 was captured when Cell 3 had the lowest voltage, thus triggering the algorithm to bleed current from Cells 1, 2 and 4. The balancing algorithm works by allowing the cells to bleed current for about 4 seconds, and resting for 1 second before determining whether balancing should continue or not. During the balancing period, the temperature of the resistors increases to 45°C, and fall back down to 42°C during the rest period. This cyclic behaviour continues while balancing is needed.



Figure 6.12: Temperature profile of bleeding resistors when cell 3 has the lowest voltage

# Chapter 7

# Conclusion and Further Work

## 7.1 Conclusion

The design of a solar-powered streetlight involves a high level system design and the implementation of individual subsystems. The selection of the PV panel, charge controller, batteries and luminaire were analysed to refine the system design. The result of the analysis is a 15W LED, 40W PV panel system that is charged in 4 hours and operates at maximum power for 8 hours.

A solar charge controller was designed and implemented, with tests validating its CC/CV and MPPT functions, and characterising its efficiency at 88%. The designs for the PCB are released as open-source and can be accessed at: <https://workspace.circuitmaker.com/Projects/Details/GraceTam-2/CCSolar>

An open sourced cell balancing and voltage reading circuit was used for the implementation of the charge controller with credit for the design going to the original work. Finally, the luminaire was designed using high efficiency COB LEDs on an aluminium-base PCB.

## 7.2 Further Work

Each subsystem was tested and validated to be working, however there was insufficient time for a full system integration and test. A full integration should be performed to evaluate the performance of the system.

The BMS that was implemented was a fallback version with much more work to be done on it. Currently, the system relies on the charge controller cutting off its charging current to prevent the batteries from being over-charged. However, this is insufficient protection as any malfunctions on the charge controller might lead to the battery being over-charged. A circuit breaker should be implemented between the positive connection of the battery pack and the top-most cell in the stack (cell 4). The current BMS already performs voltage reading, so the same microcontroller can be used to open the circuit breaker if any of the cells reach 3.65V or 2.5V. Besides that, the battery should be protected from over-current conditions where it discharges too quickly. A PTC resistor can be used as a re-settable fuse between the battery and the load, with the fuse being opened when too much current is drawn from the battery. These protections were not implemented due to a lack of time, but should be added to the circuit as future work.

During the late stages of this project, another IC was identified in addition to the ones presented in Figure 4.6. The ISL94202 by Renesas is a BMS IC that can be used in standalone mode without a host controller. The protection and cell balancing thresholds can be set using an EEPROM that is programmed once via an I<sub>2</sub>C interface. This option was only found after the BMS circuit had been implemented, so it was not pursued further due to a lack of time. However, it is in stock on major suppliers' websites and can be implemented for the BMS. The reference designs show a very simple circuit with low part count and it performs autonomous cell balancing. [64]

This project forms the groundwork for an open sourced solar streetlight design, so the cost was considered during decision making but was not the biggest priority. More work can be done on reducing the cost of the system. For example, the LED driver was purchased for £16 which is very expensive considering its simple function. The cost can be reduced if it were designed from scratch. Another way to reduce the cost of the system is to adjust the sizing of the system to have a shorter operating time. The alternative system design in Figure 7.1 would produce the same level of brightness for a reduced full operating time of 4 hours at half the cost. Conversely, the same operating time can be maintained for half the brightness.

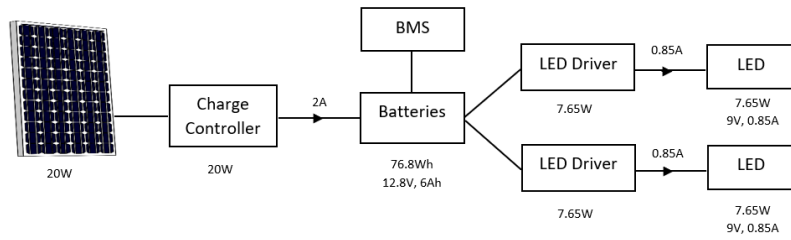


Figure 7.1: Alternative system design for reduced cost and reduced reliability

# Appendix A

## PV Panel Spice Model

The model of the solar panel provided by Analog Devices was oversized and did not have much information or instructions on editing it. To remove the ambiguity of the simulation, a single-diode PV model was designed (Figure A.1a). The 5 parameters of the circuit were obtained using the method explained in Section 4.1.2, and were implemented on the single diode schematic. The output of the PV model was plotted in Figure ?? and the results were verified to be the expected curve of a PV panel. For this simulation, a PV model was used instead of using DC values to represent the MPP of the panel so that the MPPT function of the IC could be observed.

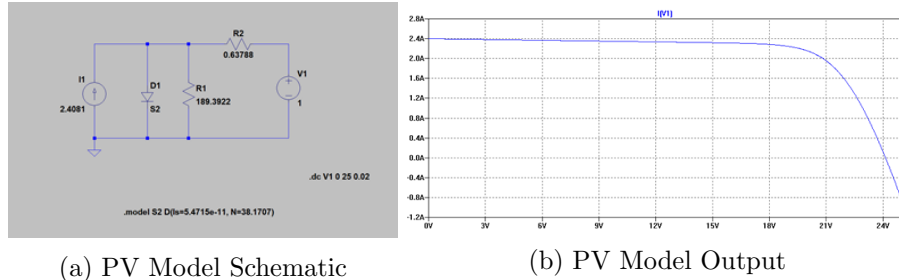


Figure A.1: Single Diode PV LTSpice Model

The resulting netlist from this PV modelling is:

```
.subckt <VALUE> K A
D1 N001 K S2
R1 N001 K 189.3922
R2 N001 A 0.63788
I1 K N001 2.4081
.model S2 D(Is=5.4715e-11, N=38.1707)
.end
```

## **Appendix B**

# **Bill of Materials**

### **B.1 Charge Controller**

The selection of the diodes in Table B.1 is credited to [60]

Identifier	Value	Mfr No
Jumper	-	1729128
LT3652	-	LT3652EDDPBF
L1	15uH	Wurth 74437346220
D1	Schottky	V4PAL45-M3/I
D2	LED	LTST C170KRKT
D3	LED	LTST C170KRKT
D4	Schottky	V4PAL45-M3/I
D5	Silicon	1N4148WS
D6	Zener	MMSZ5234BT1G
C1	10uF	GCJ31CD7YA106KE02L
C2	1uF	C0805C105M3REC7210
C3	0.68uF	C0805C684K5RACAUTO7210
C4	100uF	EEE-FN1V101XV
C5	10uF	EMK316BJ106KL8T
R1	576K	CRCW0805576KFKEA
R2	100K	CRCW0805100KFKEAC
R3	10K	CRCW080510K0FKEAC
R4	10K	CRCW080510K0FKEAC
R5 (Rsense)	0.068	WSL1206R0680FEB
R6	1.1M	ERJ6ENF1104V
R7	348K	MCWF08R3483BTL

Table B.1: Charge Controller Bill of Materials

## B.2 BMS

The selection of the resistors, diodes and capacitors in Table B.2 is credited to [51].

Comment	Designator	Quantity
100n	C1, C2, C3, C4, C5	5
1N4148	D1, D2, D3	3
Harwin M20-7822046	J1	1
Phoenix Contact 1754520	J2	1
DMG3402L-7	Q1, Q3, Q5, Q8, Q11	5
DMG2307L	Q2, Q4, Q6, Q7, Q9, Q10, Q12	7
3K	R1, R4, R6, R17, R26, R31, R34, R44	8
820	R2	1
100K	R3, R7, R14, R15, R25, R27, R30, R33, R46, R55	10
18K	R5	1
120	R8 - R13, R18 - R23, R35 - R40, R48 - R53	24
4K7	R16	1
68K	R24, R28, R29, R54	4
9K1	R32	1
31K	R41	1
39K	R42	1
91K	R43, R56	2
12K	R45	1
2K7	R47	1

Table B.2: BMS BOM

### B.3 Miscellaneous

The other components that were required for the system design are listed in Table B.3.

Identifier	Value	Mfr No	Quantity
PV Panel	20W	Monocrystalline Solar Panel Series 4a - 20W 12V	1
Microcontroller	-	Arduino Nano	1
LED Driver	1A	RCD-24-1.00/PL/A	1
LED	3.3V	XM-L2 XMLBWT-00-0000-0000U2051	3

Table B.3: Bill of Materials for the system

# Bibliography

- [1] PV Performance Modeling Collaborative, “Single diode equivalent circuit models,” accessed: 2022-1-26. [Online]. Available: <https://pvpmc.sandia.gov/modeling-steps/2-dc-module-iv/diode-equivalent-circuit-models/>
- [2] S. N. Kevin Scott, “Active battery cell balancing,” Analog Devices, Tech. Rep. [Online]. Available: <https://www.analog.com/media/en/technical-documentation/tech-articles/Active-Battery-Cell-Balancing.pdf>
- [3] Analog Devices, “Lt3652 power tracking 2a battery charger for solar power,” accessed: 2022-4-22. [Online]. Available: <https://www.analog.com/en/products/lt3652.html>
- [4] S. Trace, “South africa’s crippling electricity problem,” Oxford Policy Management, blog, Jan 2020. [Online]. Available: <https://www.opml.co.uk/blog/south-africa-s-crippling-electricity-problem>
- [5] J. Wright and J. Calitz, “Setting up for the 2020s: Addressing south africa’s electricity crisis and getting ready for the next decade... and now covid-19,” pp. 5–6, Aug 2020.
- [6] G. I. Crabb and L. Krinson, “The impact of street lighting on night-time road casualties,” in *Safer Roads Conference 2008*, 2008, pp. 2–3.
- [7] K. Jäger, O. Isabella, A. H. Smets, R. A. van Swaaij, and M. Zeman, *Solar Energy: Fundamentals, Technology and Systems*, 1st ed. Delft University of Technology, 2014.
- [8] EXC, “How to design and calculate solar powered street lamp?” EXC, Shenzhen, China, 2021. [Online]. Available: <https://www.exc-streetlight.com/news/lighting-blogs/how-to-design-and-calculate-solar-powered-street-lamp.html>

- [9] R. H. T. de Almeida, Master's thesis.
- [10] J. Fang and B. Pham, Master's thesis.
- [11] A. Junyent-Ferre, "Lecture notes on photovoltaic generation," Imperial College London, Feb 2018.
- [12] ESMAP, "Global photovoltaic power potential by country," Washington, DC: World Bank, 2020. [Online]. Available: <https://documents1.worldbank.org/curated/en/466331592817725242/pdf/Global-Photovoltaic-Power-Potential-by-Country.pdf>
- [13] S. Ahmed, A. H. Zenan, N. Tasneem, and M. Rahman, "Design of a solar powered led street light: Effect of panel's mounting angle and traffic sensing," in *2013 IEEE Conference on Sustainable Utilization and Development in Engineering and Technology (CSUDET)*, 2013, pp. 74–79.
- [14] W. Soto, S. Klein, and W. Beckman, "Improvement and validation of a model for photovoltaic array performance," *Solar Energy*, vol. 80, pp. 78–88, 01 2006.
- [15] M. M. Hoque, M. A. Hannan, and A. Mohamed, "Optimal cc-cv charging of lithium-ion battery for charge equalization controller," in *2016 International Conference on Advances in Electrical, Electronic and Systems Engineering (ICAEEES)*, 2016, pp. 610–615.
- [16] D. Grubbs, "How to select a solar charge controller," Solar Power World, 2019, accessed: 2022-1-26. [Online]. Available: <https://www.solarpowerworldonline.com/2019/12/how-to-select-a-solar-charge-controller/>
- [17] J. Dalal, H. Chandwani, T. Bhagwat, M. Karvande, and M. S. Shaikh, "Implementation of universal solar charger for ev applications using a cascaded buck-boost converter," in *2021 6th International Conference for Convergence in Technology (I2CT)*, 2021, pp. 1–6.
- [18] A. Victor, D. K. Mahato, A. Pundir, and G. J. Saxena, "Design, simulation and comparative analysis of different types of solar charge controllers for optimized efficiency," in *2019 Women Institute of Technology Conference on Electrical and Computer Engineering (WITCON ECE)*, 2019, pp. 17–21.
- [19] GRNLED, "What types of battery is the best for solar street lights?" accessed: 2022-6-2. [Online]. Available: <https://grnled.com/blog/what-types-of-battery-is-the-best-for-solar-street-lights.html>

- [20] H. Keshan, J. Thornburg, and T. S. Ustun, “Comparison of lead-acid and lithium ion batteries for stationary storage in off-grid energy systems,” in *4th IET Clean Energy and Technology Conference (CEAT 2016)*, 2016, pp. 1–7.
- [21] Dave Knight, Lithium Ion Cell Protection. [Online]. Available: <https://www.digikey.co.uk/en/maker/blogs/lithium-ion-cell-protection>
- [22] RS Pro, RS PRO, 3.2V, 18650, Lithium Phosphate Rechargeable Battery, 1.5Ah. [Online]. Available: <https://docs.rs-online.com/756f/0900766b816d2c10.pdf>
- [23] B. Yildirim, M. Elgendi, A. Smith, and V. Pickert, “Evaluation and comparison of battery cell balancing methods,” in *2019 IEEE PES Innovative Smart Grid Technologies Europe (ISGT-Europe)*, 2019, pp. 1–5.
- [24] *The Lighting Handbook*, 6th ed., Zumtobel Lighting GmbH, 4 2018.
- [25] Lumenistics, “Illuminance explained,” accessed: 2022-1-26. [Online]. Available: <https://lumenistics.com/illuminance-define/>
- [26] B. Smidt-Hart, “Public lighting, lighting the way to smart city development,” in *AMEU Convention 2019*, 2019.
- [27] “Public lighting – part 1: The lighting of public thoroughfares,” South African Bureau of Standards, Standard, 2007.
- [28] *Lighting Terminology Guide*, Genux Lighting, 2019.
- [29] “Modelling energy efficiency potential in municipal operations of the sacn member cities,” South African Cities Network, Tech. Rep., 2014.
- [30] IEA, “Lighting,” IEA, Paris, 2021. [Online]. Available: <https://www.iea.org/reports/lighting>
- [31] “Renewable energy,” Department of Mineral Resources and Energy, South Africa, accessed: 2022-1-26. [Online]. Available: [http://www.energy.gov.za/files/esources/renewables/r\\_solar.html](http://www.energy.gov.za/files/esources/renewables/r_solar.html)
- [32] Solar Streetlights Africa, “20w solar led street light,” Product datasheet.
- [33] Solux, “Optimal-one integrated solar streetlight,” Sinetech product datasheet.
- [34] Phillips Lighting, “Sunstay - all in one solar street light,” Product family leaflet, Jan 2022.

- [35] V. Energy, “Bluesolar monocrystalline panels,” Product Datasheet, accessed: 2022-1-26. [Online]. Available: <https://www.victronenergy.com/upload/documents/Datasheet-BlueSolar-Monocrystalline-Panels-EN.pdf>
- [36] Renogy, “Rng-30d-ss 30w monocrystalline solar panel,” Product Datasheet, accessed: 2022-1-26. [Online]. Available: <https://uk.renogy.com/content/files/Specifications/RNG-30D-SS-E.pdf>
- [37] R. Pro, “Mono poly-crystalline (12 volt) silicone solar cell modules,” Product Datasheet, accessed: 2022-1-26. [Online]. Available: <https://docs.rs-online.com/84a6/0900766b815873a7.pdf>
- [38] R. H. G. Tan and M. Y. W. Teow, “A comprehensive modelling of photovoltaic module characteristic curve in matlab/simulink,” in *4th IET Clean Energy and Technology Conference (CEAT 2016)*, 2016, pp. 1–6.
- [39] A. Ilyas, M. R. Khan, and M. Ayyub, “Lookup table based modeling and simulation of solar photovoltaic system,” in *2015 Annual IEEE India Conference (INDICON)*, 2015, pp. 1–6.
- [40] T. Huld, R. Müller, and A. Gambardella, “A new solar radiation database for estimating pv performance in europe and africa,” *Solar Energy*, vol. 86, p. 1803–1815, 06 2012.
- [41] S. A.-H. Greg Albright, Jake Edie, “A comparison of lead acid to lithium-ion in stationary storage applications,” AllCell Technologies LLC, Standard, 2012.
- [42] Victron Energy VE.Bus BMS – BMS300200000. [Online]. Available: <https://www.batterymegastore.co.uk/product/victron-energy-ve-bus-bms300200000/>
- [43] T. Instruments, BQ77905. [Online]. Available: <https://www.ti.com/product/BQ77905>
- [44] STMicroelectronics, Datasheet - L9963E - Automotive Multicell battery monitoring and balancing IC. [Online]. Available: <https://www.mouser.co.uk/datasheet/2/389/dm00768850-2583045.pdf>
- [45] T. Instruments, BQ76925. [Online]. Available: <https://www.ti.com/product/BQ76925>
- [46] Analog Devices, LTC6810-1. [Online]. Available: <https://www.analog.com/en/products/ltc6810-1.html#product-overview>

- [47] Texas Instruments, BQ769142. [Online]. Available: <https://www.ti.com/product/BQ769142>
- [48] T. Instruments, BQ77PL900. [Online]. Available: <https://www.ti.com/product/BQ77PL900>
- [49] Texas Instruments, BQ76942. [Online]. Available: <https://www.ti.com/product/BQ76942>
- [50] T. Instruments, BQ77915. [Online]. Available: <https://www.ti.com/product/BQ77915>
- [51] D. Moniatis, “Design of a battery management system and a communication system for the open source wheelchair project,” Master’s thesis, 2020.
- [52] “Victron mppt charge controllers,” accessed: 2022-5-30. [Online]. Available: [https://www.batteriesandsolar.co.uk/shop-categories/smartsolar-mppt-100-20\\_48v-retail/](https://www.batteriesandsolar.co.uk/shop-categories/smartsolar-mppt-100-20_48v-retail/)
- [53] U. Mohammed, M. A. Aminu, S. A. Adeshina, O. Oshiga, G. Koyunlu, and S. Thomas, “Design and implementation of regulated dc variable power supply using solar pv with storage (0-15v, 5a),” in *2019 15th International Conference on Electronics, Computer and Computation (ICECCO)*, 2019, pp. 1–6.
- [54] Texas Instruments, “Mppt charge controller reference design for 12-v, 24-v and 48-v solar panels,” Design Guide: TIDA-010042, Jan 2020.
- [55] Cree, Cree® XLamp® XM-L2 LEDs. [Online]. Available: <https://docs.rs-online.com/cf93/0900766b816f243d.pdf>
- [56] Texas Instruments, LM3405A 1.6-MHz, 1-A Constant Current Buck LED Driver With Internal Compensation in Tiny SOT and MSOP-PowerPAD™ Packages. [Online]. Available: <https://www.ti.com/lit/ds/snvs508d/snvs508d.pdf>
- [57] Recom, Constant Current LED Driver. [Online]. Available: <https://docs.rs-online.com/05c5/0900766b81373236.pdf>
- [58] Analog Devices, *LT3652*, Power Tracking 2A Battery Charger for Solar Power. [Online]. Available: <https://www.analog.com/media/en/technical-documentation/data-sheets/3652fe.pdf>

- [59] Sparkfun, SparkFun Sunny Buddy - MPPT Solar Charger. [Online]. Available: <https://www.sparkfun.com/products/12885>
- [60] Craig Peacock, SOLAR POWER CHARGER 2A LITHIUM SLA. [Online]. Available: <https://circuitmaker.com/Projects/Details/Craig-Peacock-4/Solar-Power-Charger-2A-Lithium-SLA>
- [61] Cree, “Optimizing pcb thermal performance for xlamp® leds,” PRODUCT DESIGN GUIDE. [Online]. Available: <https://docs.rs-online.com/cf93/0900766b816f243d.pdf>
- [62] Analog Devices, DEMO MANUAL DC1568A. [Online]. Available: <https://www.analog.com/media/en/technical-documentation/user-guides/dc1568afa.pdf>
- [63] Z. Pantely, “Battery emulation for charger evaluation,” Analog Devices, Tech. Rep. [Online]. Available: [https://ez.analog.com/cfs-file/\\_key/communityserver-discussions-components-files/330/2821.Battery-Emulation-for-Charger-Evaluation.pdf](https://ez.analog.com/cfs-file/_key/communityserver-discussions-components-files/330/2821.Battery-Emulation-for-Charger-Evaluation.pdf)
- [64] Renesas, ISL94202 Datasheet. [Online]. Available: <https://www.renesas.com/eu/en/document/dst/isl94202-datasheet?r=507571>